Inhibition of the H3K27 demethylase UTX enhances the epigenetic silencing of HIV proviruses and induces HIV-1 DNA hypermethylation but fails to permanently block HIV reactivation

Kien Nguyen*, Curtis Dobrowolski[#a], Meenakshi Shukla, Won-Kyung Cho[#b], & Jonathan Karn

Department of Molecular Biology and Microbiology, Case Western Reserve University Medical School, Cleveland, Ohio, United States of America

[#a]Current address: Wallace H. Coulter Department of Biomedical Engineering, Georgia Institute of Technology and Emory School of Medicine, Atlanta, Georgia, United States of America

[#b] Korean Medicine (KM)-Application Center, Korea Institute of Oriental Medicine (KIOM), 70 Cheomdan-ro, Dong-gu, Daegu 41062, Republic of Korea

*Corresponding author

E-mail: Kien.Nguyen@case.edu

Short Title: Enhanced histone and DNA methylation does not block HIV reactivation

Abstract

One strategy for a functional cure of HIV-1 is “block and lock”, which seeks to permanently suppress the rebound of quiescent HIV-1 by epigenetic silencing. For the HIV LTR, both histone 3 lysine 27 tri-methylation (H3K27me3) and DNA methylation are associated with viral suppression, while H3K4 tri-methylation (H3K4me3) is correlated with viral expression. However, H3K27me3 is readily reversed upon activation of T-cells through the T-cell receptor. To suppress latent HIV-1 in a stable fashion, we depleted the expression or inhibited the activity of UTX/KDM6A, the major H3K27 demethylase, and investigated its impact on latent HIV-1 reactivation in T cells. Inhibition of UTX dramatically enhanced H3K27me3 levels at the HIV LTR and were associated with increased DNA methylation. In latently infected cells from patients, GSK-J4, which is a potent dual inhibitor of the H3K27me3/me2-demethylases JMJD3/KDM6B and UTX/KDM6A, effectively suppressed the reactivation of latent HIV-1 and induced DNA methylation at specific sites in the 5’LTR of latent HIV-1 by the enhanced recruitment of DNMT3A to HIV-1. Nonetheless, suppression of HIV-1 through epigenetic silencing required the continued treatment with GSK-J4 and was rapidly reversed after removal of the drug. Thus, epigenetic silencing by itself appears to be insufficient to permanently silence HIV-1 proviral transcription.

Author Summary

The “block and lock” strategy for a functional HIV-1 cure is based on the premise that permanent inactivation of the HIV-1 can be achieved by epigenetic silencing of the proviral DNA. For cellular genes, long-term silencing is achieved during cell differentiation by the induction of specific epigenetic modifications involving histone and DNA methylation. During HIV-1 silencing, histone methylation and DNA methylation are observed, but both sets of modifications can be reversed upon activation of T-cells through the T-cell receptor or potent latency reversing agents. In an attempt to enhance silencing of HIV-1 transcription, we used an inhibitor of H3K27 demethylases to increase H3K27 methylation. This in turn led to enhanced DNA methylation of HIV-1. Unfortunately, although the treatment effectively silenced HIV-1 and prevented viral reactivation, the silencing effects were short-lived and quickly reversed after removal of the drug.

Introduction

Despite effective long-term suppression of viral loads by combination antiretroviral therapy (cART), latent HIV-1 may quickly rebound upon cessation of treatment [1, 2]. There are two major strategies for eliminating latent proviruses. The first, often referred to as “kick and kill” [3], is based on the concept that latent HIV-1, once pharmacologically reactivated by latency reversing agents (LRAs), could subsequently be eliminated by cytotoxicity and/or the enhanced immunological surveillance [4, 5]. Unfortunately, “kick and kill” faces formidable challenges in achieving reactivation of the majority of latent provirus [6-10] and difficulties in inducing HIV-1 specific immune-mediated clearance *in vivo* [11-13]. An alternative approach, referred to as “block and lock”, is designed to permanently suppress the rebound of quiescent HIV-1 by inducing epigenetic silencing [14-16]. In the best documented example of a “block and lock” strategy, the Valente laboratory has reported that didehydro-cortistatin A (dCA), an inhibitor of HIV-1 transcription can enhance epigenetic silencing of the HIV-1 promoter, leading to long-term inactivation of the provirus [17-20]. Regardless of the chosen strategy, a more comprehensive understanding of the mechanism involved in HIV-1 latency is urgently required when designing effective HIV-1 cure strategies.

Multiple complementary molecular mechanisms contribute to the development of HIV-1 latency in T-cell populations, including sequestration of key transcription initiation and elongation factors [21]. In addition, numerous epigenetic modifications of histones on the HIV-1 LTR, including H3K27 and H3K9 methylation, serve to silence HIV-1 proviruses [22-29].

H3K27 trimethylation (H3K27me3) provides one of the essential silencing mechanisms of HIV-1 in $CD4^+$ T cells [23, 24, 30-33]. EZH2, the enzymatic moiety of the polycomb repressive complex 2, is the sole H3K27 methyltransferase (H3K27MT) in mammalian cells. Opposing the H3K27MT is UTX/KDM6A, one of two specific H3K27 demethylases, containing highly homologous Jumonji C domains [34, 35], that selectively demethylates H3K27me3 and H3K27me2. UTX is essential for the activation of transcriptionally repressed genes containing bivalent promoters [36, 37]. UTX is a component of the UTX-MLL2/3 complexes, which maintain the transcriptionally positive epigenetic mark H3K4me3.

In addition to histone methylation, promoters are often permanently silenced by DNA methylation, which occurs when cytosine residues are methylated by DNA methyltransferases (Dnmts) to create 5-methylcytosine (5mC) residues [38]. The majority of DNA methylation occurs at cytosine in the CpG islands [39]. Methylated DNA itself suppresses the transcription of cellular genes by eliminating the binding of transcription activators [38]. In addition, methylation of DNA also promotes the binding of methylated-DNA binding proteins which usually function as transcription co-repressors [38, 40, 41]. DNA methylation of CpG islands in the promoter is usually associated with long-term transcription repression [42].

DNA methylation at two CpG islands flanking the transcription start site in the HIV-1 5' LTR has been associated with HIV-1 silencing [43, 44]. However, the latent viral reservoir of HAART-treated aviremic patients displays very low or no DNA methylation suggesting that direct DNA modification is not a major control mechanism for latency [45, 46].

We reasoned that since H3K27me3 is essential for HIV-1 latency in T cells [23, 24] enhancement of H3K27me3 by inhibition of H3K27 demethylases, particularly UTX, could lead to permanent silencing of the provirus. Blocking UTX was able to prevent proviral reactivation and led to increases in both H3K27me3 and DNA methylation at specific sites in the 5' LTR. Unfortunately, this did not result in irreversible suppression of latent HIV-1 in T cells, suggesting that epigenetic silencing is short-lived and cannot by itself lead to a permanent block to HIV-1 rebound.

Results

Depletion of UTX expression blocks HIV-1 reactivation

UTX/KDM6A is a specific H3K27 demethylase that selectively targets H3K27me3 and H3K27me2. Since H3K27me3 formation by EZH2 is a powerful repressive mechanism to silence HIV-1 [23, 24], we reasoned that knockdown of UTX could be used to enhance HIV-1 transcriptional silencing and perhaps establish a permanently silenced provirus. As shown in **Fig 1**, we initially performed knockdown studies in the latently infected Jurkat E4 cell line [23, 24, 47] using two different shRNAs designed to target UTX (shUTX(1) & shUTX(2)) along with a scrambled shRNA control. The shRNAs were introduced into the E4 cells using a lentiviral expression vector and single cells were then sorted into wells to derive clones. As shown in **Fig 1A & B**, after reactivation of the latent proviruses by TNFα stimulation, up to 76% GFP+ cells were obtained in the cells expressing the scrambled shRNA control, while we observed less than 30% viral reactivation in two representative clones expressing two different shRNAs to UTX (shUTX-cl1; shUTX-cl2). We observed similar blocks to HIV-1 reactivation by SAHA or T cell receptor (TCR) activation (**Fig 1B**). In addition, we confirmed the inhibitory effect of UTX knockdown on HIV-1 using two other latently infected Jurkat cell lines: 3C9 cells, harboring Nef+ wild-type Tat HIV-1, and 2D10 cells, infected with Nef- H13L Tat HIV-1 (**Fig 1B**).

To verify that the inhibition on HIV-1 reactivation was not clonally dependent, multiple clones of E4 cells transduced with either the scrambled or UTX shRNAs were reactivated using 2 μM of SAHA overnight (**Fig 1C**). Expression of both UTX shRNA sequences not only significantly inhibited the basal transcription of provirus but also

prevented proviruses from being reactivated by SAHA stimulation, although the shUTX(2) sequence was somewhat less efficient than shUTX(1) in reducing expression levels of HIV-1.

The relative potency of the two shRNAs was verified by Western blots using a specific UTX antibody (**Fig 1D**). UTX levels were depleted by more than 70% using both UTX shRNAs, with shUTX(1) showing somewhat greater activity than shUTX(2), consistent with their relative activity in inducing HIV-1 transcriptional blocks. As expected, UTX depletion also resulted in elevation of cellular H3K27me3 levels.

In summary, we were able to demonstrate in three latently infected Jurkat T-cell lines and in multiple clones derived from two unique shRNAs that UTX depletion enhances HIV-1 silencing and blocks reactivation of HIV-1 transcription.

Enhanced recruitment of UTX to the HIV-1 LTR during proviral reactivation

UTX activates HIV-1 provirus by converting the LTR chromatin structure to a more transcriptionally active state by up-regulation of H3K4 methylation and down-regulation of H3K27 methylation [48]. We confirmed and expanded these observations using chromatin immunoprecipitation (ChIP) assays [23, 24, 49] to measure the accumulation of RNAP II, UTX, EZH2 and H3K27me3 at the 5'LTR of reactivated proviruses (**Fig 2**).

After stimulation of latent proviruses with 10 ng/ml TNF-α for an hour, we observed a more than 10-fold increase in RNAP II recruitment to the Nuc-0, promoter, and Nuc-1 regions of HIV-1 5'LTR (**Fig 2A**), indicating the initiation of viral transcription. The increase in RNAP II was associated with a 2 to 3-fold elevation of UTX (**Fig 2B**). Consistent with our previous reports documenting EZH2 repression of HIV-1 transcription in T cells [23, 24], proviral reactivation resulted in corresponding reductions in the levels of EZH2 (**Fig**

2C) and H3K27me3 (**Fig 2D**). ChIP assays were also performed on an E4 clone expressing shUTX(2) RNA and a control clone expressing the scrambled shRNA. Depletion of UTX resulted in a reduction of RNAP II occupancy throughout the LTR (**Fig 2E**). The expected removal of UTX throughout the HIV-1 provirus was demonstrated as a control for shRNA potency (**Fig 2F**). Together, our data demonstrates that UTX is recruited to HIV-1 5'LTR and facilitates the initiation of HIV-1 transcription.

The HIV-1 LTR is a bivalent promoter and requires UTX for reactivation

Bivalent promoters, which include the HIV-1 LTR [48], characteristically contain both activating H3K4me3 and repressive H3K27me3 marks at the same nucleosomes and are usually maintained at a repressed but inducible transcriptional state [50, 51]. The important role of UTX demethylase activity for the resolution and activation of genes containing bivalent promoters has been documented [36, 37].

To directly evaluate whether the UTX demethylase activity participates in HIV-1 transcriptional reactivation, we inhibited H3K27me3 using GSK-J4, a specific antagonist for both UTX and JMJD3 demethylase activity. E4 and 3C9 cells were pretreated for 24 hours with 5 or 10 μM of GSK-J4, then further stimulated with 2 μM SAHA or 10 ng/ml TNFα overnight. As shown in **Fig 3A**, a dose-dependent inhibition of HIV-1 reactivation was observed in both E4 and 3C9 cells when cells were treated with GSK-J4. This was seen in all tested concentrations of SAHA and TNFα. With 10 μM of GSK-J4, a maximal reduction of more than 50% in the reactivation levels of provirus was obtained in both cell lines. Representative histograms showing the FACS analysis of HIV-1 reactivation are shown in **S1 Fig**.

ChIP performed on E4 cells measuring the density of RNAP II, H3K4me3, and H3K27me3 at the 5'LTR of silenced provirus confirms the bivalent nature of the HIV-1 promoter and the ability of GSK-J4 to block proviral reactivation (**Fig 3B to D**). In untreated cells, RNAP II accumulates near the promoter and Nuc-1 (**Fig 3B**) [49]. Nuc-1 and Nuc-2 are simultaneously occupied by both methylated histones (**Fig 3C & D)** [48].

Upon TNF-α stimulation in the absence of GSK-J4, there was enhanced recruitment of RNAP II to HIV-1 promoter region (-116 to +4 position relative to transcription start site (TSS)), a direct measure of transcriptional reactivation of HIV-1 [49]. Concomitantly, H3K4me3 levels at the Nuc-1 and Nuc-2 regions were substantially increased, and as expected, H3K27me3 was completely removed at the same regions [23, 24]. By contrast, when the provirus was reactivated by TNF-α in the presence of GSK-J4, the levels of H3K4me3 and H3K27me3 were fully restored, while RNAP II levels were reduced (**Figs 3B to D**).

These observations strongly support the conclusion that the H3K27 demethylase activity of UTX is essential for the reactivation of the silent provirus' bivalent 5'LTR.

Simultaneous demethylation of H3K27me3 and methylation of H3K4 are required for HIV-1 reactivation

The bivalency of the HIV-1 5' LTR and the association of UTX with the H3K4 methyltransferase MLL2/MLL3 complex strongly suggested that H3K4me3 is crucial for HIV-1 reactivation. To test this hypothesis, we ectopically expressed HA-tagged histone H3.3 containing either a wild type sequence, the single mutants K4M and K27M, or a double mutant K4M-K27M and investigated their impacts on HIV-1 reactivation. Lysine to methionine (K to M) mutations of H3.3 have dominant negative effects on the global lysine

197 methylation of histone H3 at different residues [52]. A substantial reduction in the cellular
198 levels of H3K27me3 or H3K4me2-3 was observed in cells expressing K4M or K27M
199 mutants of H3.3 (**Fig 4A**). Compared to the wild type, the K27M mutant spontaneously
200 reactivated HIV-1 and significantly sensitized provirus to reactivation induced by 2 μM
201 SAHA or 10 ng/ml TNF-α. By contrast, the K4M mutant had no significant effect on HIV-
202 1 reactivation (**Fig 4B**). The double mutant K4M-K27M abolished the enhanced
203 reactivation induced by the K27M single mutant and restored the phenotype of wild type
204 H3.3 (**Fig 4B**).

205 We conclude that maintenance of H3K4me3 is required for the reactivation of HIV-
206 1 transcription mediated by the demethylation of H3K27me3. This strongly indicates that
207 UTX plays a dual role in HIV-1 reactivation: removal of H3K27me3 and recruitment of
208 MLL2/3 complexes to deposit H3K4me3.

209 **Inhibition of UTX induces DNA methylation of the HIV-1 LTR**

210 DNA methylation is generally a more permanent epigenetic silencing mechanism
211 than histone methylation alone. Often during development, increases of H3K27
212 methylation result in a corresponding increase in DNA methylation leading to permanent
213 gene silencing [53-55]. Since, depletion of UTX caused an increase in global H3K27me3
214 levels, we next tested whether UTX depletion also induce DNA methylation of HIV-1.

215 The HIV-1 genome carries a series of CpG islands that are subject to DNA
216 methylation (**Fig 5A**), although the functional role of DNA methylation in HIV-1 latency is
217 controversial [45, 56-58]. One commonly used approach for measuring the impact of DNA
218 methylation on gene expression is to use 5'-Azacytidine (5-AZC), an analogue of cytosine
219 that can be incorporated into DNA during DNA replication, to inhibit DNA

methyltransferases (DNMTs). Binding of DNMTs to 5-AZC results in "covalent trapping" of DNMTs resulting in degradation of the enzymes [59]. An increase in gene expression by 5-AZC therefore implies removal of a repressive DNA methylation mark. As shown in **Fig 5B**, E4 cells expressing either scrambled or UTX shRNAs were treated for 72 hours with 5-AZC (1 μM), then left untreated or stimulated further overnight either through the T-cell receptor (TCR) (using as combination of α-CD3 (125 ng/ml) and α-CD28 (500 ng/ml)), treatment with 500 nM of SAHA, or activation with 1 ng/ml of TNF-α. HIV-1 transcription was measured by monitoring d2EGFP expression levels using flow cytometry. Compared to the scrambled shRNA-treated control cells, we observed greater elevations of HIV-1 expression in the shUTX knock down cells. When treated with 5-AZC, cells expressing scrambled shRNA showed a less than a 1.5-fold increase in HIV-1 expression while the UTX shRNA treated cells resulted showed a 3 to 6-fold increase. Reactivation of the proviruses following treatment of 5-AZC pretreated cells through the TCR, SAHA, or TNF-α each enhanced reactivation of HIV-1 in shUTX knock down cells compared to the control cells.

In a complementary approach, we directly measured the levels of 5'-methylcytosine at the HIV-1 provirus in a E4 clone expressing UTX-1 shRNA by MeDIP coupled to qPCR. The primers used for qPCR (**Fig 5A**) were designed to specifically amplify the 5' CpG, NCR CpG and Env CpG islands [60]. However, the Nuc-2 primers used in this study only covered the downstream region of NCR CpG cluster. Compared to HIV-1 from control cells, HIV-1 from the shUTX knock down cells contained much higher levels of 5'-methylcytosine. Similarly, HIV-1 from E4 cells treated with GSK-J4 also

contained higher levels of DNA methylation at the 5' CpG and Nuc-2 clusters than HIV-1 proviruses from untreated cells (**Fig 5C**).

Taken together, our data demonstrate that either the depletion of UTX by shRNA or inhibition of its demethylase activity by GSK-J4 greatly increased the DNA methylation of HIV-1 proviruses.

DNMT3A is recruited to the HIV-1 LTR after inhibition of UTX by GSK-J4

To further study the interplay between UTX and DNA methylation, we ectopically expressed the transgene DNMT3A-3xFlag. In this construct, 3xFlag was introduced at the C-terminal of DNMT3A which allowed us to perform ChIP assays using the Flag M2 antibody to measure the enrichment of DNMT3A at HIV-1 5'LTR. E4 cells transduced with *Dnmt3a*-3xFlag lentiviruses expressed greatly increased levels of DNMT3A (**Fig 5D)**. ChIP assays showed that treatment of these cells with 10 μM GSK-J4 for 48 hours resulted in significant recruitment of DNMT3A to HIV-1 5' CpG and Nuc2 clusters (**Fig 5D**), but not to the promoters of two control genes, TNFA and GAPDH. Finally, as a complementary approach we also knocked out the DNA demethylases TET1 or TET2 using CRISPR-Cas9. Knock out of either gene partially inhibited HIV-1 reactivation in Jurkat cells after reactivation with SAHA or TNF-α (**Fig 5E**). In conclusion, inhibition of UTX results in specific recruitment of DNMT3A to HIV-1, which in turn elevates DNA methylation of the HIV-1 provirus and enhances HIV-1 silencing.

Inhibition of UTX accelerates silencing of HIV-1 in primary cell models of HIV-1 latency

Epigenetic silencing in primary cells involves additional important mechanisms that are not well represented in the transformed Jurkat cell background. Specifically, we

showed previously that both the EZH2 and EHMT2 histone methyltransferases strongly restrict HIV-1 transcription in primary T-cell models for HIV-1 latency and in resting memory T-cells isolated from HIV-1 infected patients. However, EZH2 is the dominant histone methyltransferase in Jurkat T-cells and EHMT2 makes only a small contribution to silencing [23]. We therefore extended our study of the role of the H3K27 demethylase activity of UTX on HIV-1 silencing and reactivation using the well-established QUECEL (Th17 cells) primary cell model of HIV latency [22, 61] (**Fig 6**).

As outlined in **Fig 6A**, naïve CD4+ T cells obtained from 4 different donors were polarized to a Th17 phenotype and then infected with a single round HIV-1 reporter expressing d2EGFP, following the QUECEL protocol [22]. Three days after HIV-1 infection (Day 0), the cells were grown in the presence of 1 μM of GSK-J4 for 4 days, with fresh media containing the drug added after 2 days. On average, the addition of GSK-J4 increased global levels of H3K27me3 more than two fold from 4 different donors (**Fig 6B**).

At Day 0, the infected cells were transferred to media containing low concentrations of IL-2 (15 IU/ml), and IL-23 (12.5 μg/ml). The levels of d2EGFP expression were measured by flow cytometry at days 4, 6, or 8 to monitor HIV silencing. In the presence of these low concentrations of cytokines, cells gradually enter quiescence leading to silencing of HIV-1 transcription (**Fig 6C**). The extent of HIV silencing is significantly enhanced by GSK-J4. At Day 4, the average d2EGFP expression from 4 donors was 46.5% relative to day 0 (ranging from 35.5% to 54.6%) while the average d2EGFP expression from the untreated cells was 59% (ranging from 41.6% to 68.3%). The differences in the average d2EGFP expression between cells treated with GSK-J4 and untreated cells were progressively increased by Day 6 (34.5% vs 54.2%) and Day 8

(26.2% vs 47.9%) (**Fig 6C**). To confirm that the populations of GFP-negative cells were latently infected, the cell populations at Day 8 were reactivated using a combination of SAHA (1 μM) and IL15 (10 ng/ml), which is a potent reactivation condition for primary cells, [22] (**Fig 6C**).

HIV-1 DNA methylation was also measured by MeDIP at Day 4. Prior to treatment with GSK-J4, 5'-methycytosine was not detected at the 5' CpG and NCR CpG clusters in each of the 4 different donors, suggesting that there was no DNA methylation of HIV-1 at these regions under these conditions. Substantial increases in the levels of DNA methylation at these CpG clusters were detected after treatment with 1 μM GSK-J4 (**Fig 6D**). Increasing in DNA methylation of HIV-1 was statistically more significant at the 5' CpG region, the region upstream of HIV-1 TSS which also overlaps with a wide variety of transcription factors binding sites.

Since UTX is necessary for the reactivation of latent HIV-1 in Jurkat T cells, its role in the reactivation of latent HIV-1 in primary Th17 cells was also investigated by pretreatment of the cells with increasing concentrations of GSK-J4 for 48 hours prior to reactivation. Treatment of the control cells with Dynabeads reactivated more than 50% of latent viruses (from 21% to 77% d2EGFP). However, only 17% and 4% of latent viruses were reactivated in cells treated with 2 μM and 4 μM of GSK-J4, respectively. Similar results were also obtained when cells were treated with a combination of SAHA and IL-15. Quantification of data from 3 different experiments on the same donor also showed a similar result; GSK-J4 significantly inhibited the reactivation of latent HIV-1 in Th17 primary cells (**Fig 6E**). In conclusion, UTX diminishes the entry of HIV-1 into latency and is required for the reactivation of latent HIV-1 in primary Th17 cells.

GSK-J4 suppresses HIV-1 reactivation in CD4+ memory T cells isolated from HIV-1 infected donors

To investigate the impact of GSK-J4 on reactivation of latent HIV-1 in CD4+ memory T cells obtained from patients, we obtained blood samples from 5 well-suppressed HIV-1 donors and frozen PBMCs from 1 donor who underwent leukapheresis. The purified memory cells were treated with 5 μM GSK-J4 for 3 days (**Fig 7A**). The cells were then treated with Dynabeads® Human T-Activator CD3/CD28 over night to reactivate latent HIV-1. We measured HIV-1 reactivation by EDITS assays [61] (**Fig 7B**). GSK-J4 significantly inhibited the reactivation of latent HIV-1 in CD4+ memory T cells, with only about 30% of reactivation observed compared to untreated cells. As a control, the expression levels of CD69, measured by FACS as an indicator for global T cell activation, were uniformly greater than 80%, as expected (**Fig 7C**). This data also demonstrated that the inhibition of latency reversal by GSK-J4 was specific, since bystander cells treated with GSK-J4 expressed comparable levels of CD69 compared to the untreated cells after TCR stimulation (**Fig 7C**). There was also a small but statistically significant increase in H3K27me3 expression in the treated cells, and a correlation between variations in the inhibition levels of GSK-J4 on HIV-1 reactivation and H3K27me3 levels between the different donors (**Fig 7D**). Differences in the reactivation levels of untreated and GSK-J4 treated latent viruses were not due to toxicity of the compound because there was no significant decrease in cell viabilities (**Fig 7E**). Therefore, similar to the primary T cell model, reactivation of latent HIV-1 in CD4+ memory T cells from HIV-1 infected donors was also blocked by GSK-J4.

GSK-J4 induces transient HIV-1 DNA hypermethylation in CD4+ memory T cells isolated from HIV-1 infected donors

The ability of GSK-J4 to induce DNA methylation of latent HIV-1 was investigated in CD4+ memory T cells. Because of the low frequency of latently infected cells in the patient samples, HIV-1 DNA methylation was measured by targeted next-generation bisulfite sequencing on proviral DNA isolated from the same donors used in the latency reversal experiments.

The 5'LTR CpG contains nine different CpG dinucleotides. Their positions relative to HIV-1 transcription start site are shown in **Fig 8A**. Due to limitations in the amount of HIV-1 DNA, we only investigated DNA methylation of the 5'LTR CpG cluster, which is the most relevant to transcriptional control of HIV-1 [62]. As shown in **Fig 8B**, GSK-J4 increased average HIV-1 DNA methylation (CpG 1 to 9) for all tested donors and CpG1-specific methylation for 5 out of 6 donors. Untreated donors showed barely detectable levels of DNA methylation of latent HIV-1 (mean of the average levels was 0.7%), consistent with the paucity of HIV-1 DNA methylation at the same region reported from many studies [62-65]. Upon GSK-J4 treatment, a 1.3 to 10-fold (average of 3-fold) increase in the average DNA methylation was observed from all tested donors. This is inversely correlated with inhibitions of HIV-1 reactivation measured by EDITS assays in the same donor (**Fig 7B & 8B**). Interestingly, out of the nine CpG islands analyzed, we consistently detected the highest increase of methylation at CpG-1 in 5 out of 6 donors **(Fig 8C)**, while changes of methylation at the other CpG islands were very modest. An average of 4-fold increase in the DNA methylation levels was observed at CpG-1.

We next investigated whether DNA methylation at 5'LTR of HIV-1 induced by GSK-J4 could be maintained after GSK-J4 withdrawal. CD4+ memory T cells from a different batch of three HIV-1 infected donors were treated with 5 μM of GSK-J4. After 72 hours, a portion of cells was collected for next-generation bisulfite sequencing. Media containing GSK-J4 from the remaining cells was washed away and cells were cultured for additional 72 hours in media without GSK-J4. The DNA methylation levels at 5'LTR of HIV-1 from three different donors before and after GSK-J4 removal were presented in **Fig 8C**. Similar to what we showed previously, DNA methylation at 5'LTR of HIV-1 was significantly increased with an average of 4 fold by GSK-J4 treatment. After GSK-J4 removal, DNA methylation levels at HIV-1 5'LTR were restored back to the initial very levels seen in untreated cells.

Discussion

UTX is required for HIV-1 reactivation

UTX is a specific H3K27 demethylase, associated with the MLL2 and MLL3 containing complexes [66], which are responsible for H3K4 methylation. The combined reduction of H3K27me3 levels and increase in H3K4me3 levels provides a key step in the transcription activation of bivalent promoters. Our earlier studies clearly demonstrated that EZH2, the enzymatic subunit of the PCR2 complex, is required for H3K27me3 formation and is an essential silencing factor for HIV-1 transcription [23]. We reasoned that blocking UTX might enhance H3K27me3 accumulation at HIV-1 genome and block proviral reactivation. Consistent with this hypothesis, Zhang et. al [48] showed that UTX was an activator for the transcription of HIV-1 LTR-driven luciferase in TZM-bl cell, a Hela cell line harboring an integrated copy of LTR-luciferase [67].

Using a wide variety of approaches to block UTX function in multiple HIV-1 latently infected Jurkat T-cell lines, primary cells and latently infected cells obtained from patients, we demonstrate here that UTX is an essential activator for latent HIV-1 reactivation. Depletion of UTX by shRNA (**Fig 1**) or inhibition of its activity by GSK-J4 prevents the transcription of latent provirus both in Jurkat T cells (**Fig 3A**) and resting $CD4^+$ T cells cultured *ex vivo* (**Fig 6E**).

Importantly, pharmacological inhibition of UTX enzymatic activity by GSK-J4 performed on CD4+ memory T cells isolated from well-suppressed HIV-1 infected donors significantly reduces the induction of HIV-1 reactivation by TCR stimulation (**Fig 7B**). GSK-J4 also accelerates the silencing of provirus in primary Th17 cells (**Fig 6A to C**).

Finally, the inhibition of HIV-1 reactivation by GSK-J4 or UTX depletion by shRNA is observed in cells infected with wild type, H13L Tat, or Nef-deleted mutants of HIV-1 (**Fig 1**). This suggests that UTX activation of HIV-1 transcription is due to epigenetic transcriptional activation of the HIV LTR and is independent of Nef or Tat function.

UTX is required to resolve the bivalent chromatin at the 5'LTR of latent HIV-1 proviruses

Genome-wide chromatin immunoprecipitation studies have described bivalent genes, in which co-occurrence of H3K27me3, a repressive mark, and H3K4me3, an activating mark, is detected within a nucleosome [68, 69]. Bivalent genes are therefore maintained in a poised or reversibly silent state that could be promptly and forcefully activated with an appropriate signal [50]. However, the stimulus signal threshold required for full activation of bivalent genes is thought to be higher than other genes [50].

The 5' LTR of latent HIV-1 in T cells closely resembles cellular bivalent genes [50] and is characterized by the presence of H3K4me3 and H3K27me3 (**Figs 3B to 3D**), restricted transcription by PRC2 [23], and high enrichment of CpG dinucleotides [70] but low methylation of DNA regions surrounding the transcription start site (**Figs 5C & 8B**) [71, 72]. Bivalency is also consistent with robust reactivation of HIV and the extensive limitation of viral transcription elongation (**Figs 2 & 3**) [21, 23, 24, 49, 61].

UTX recruitment to the HIV-1 LTR is enhanced when latent HIV-1 is reactivated by TNFα (**Fig 2**). This alters the balance between H3K27me3 and H3K4me3 at the LTR after reactivation (**Figs 3B to 3D**). Inhibition of UTX by GSK-J4 blocks the H3K27me3 reduction and H3K4me3 increases at the HIV-1 LTR (**Figs 3B to 3D**), which correlates with the inhibition of HIV-1 reactivation in Jurkat T cell (**Fig 3A**).

411 The functional significance of H3K27me3 and H3K4me3 is confirmed using ectopic
412 expression of H3.3 variants carrying mutations at K27 and K4. These experiments shows
413 that HIV-1 reactivation mediated by H3.3 K27M is inhibited by H3.3 K4M, consistent with
414 the bivalency of its 5'LTR. The bivalency of the HIV promoter may also explain why
415 permanent suppression of the provirus is difficult to achieve.

416 This entire process is orchestrated by UTX, which combines its intrinsic H3K27
417 demethylase activity and its association with the MLL2/MLL3 complexes. The
418 requirement for UTX to induce transcription of cellular bivalent genes has been well
419 documented [36, 37], and is similar to HIV-1, as reported in this study. We hypothesize
420 that the changes in chromatin modifications at 5'LTR of latent HIV-1 are biphasic.
421 H3K27me3 removal occurs in the first phase and is required for a second phase of
422 H3K4me3 accumulation. These conclusions are further strengthened by the observation
423 that H3.3 K4M inhibits H3.3 K27M mediated HIV-1 reactivation (**Fig 4**). Therefore, our
424 ectopic expression experiments suggest that both H3K27me3 displacement and
425 H3K4me3 deposition on the same nucleosome, and possibly on the same histone H3
426 subunits, are required for efficient reactivation of latent HIV-1.

427 **Transient DNA methylation of latent HIV-1 is induced by inhibition of UTX**

428 The interplay between H3K27me3 and DNA methylation has not been fully
429 elucidated. Genome-wide studies mapping overlapping sites of H3K27me3 by ChIP-seq
430 and methylated CpG microarray data reveal a mutually exclusive relationship between
431 these two marks at CpG promoters [73-75]. However, some studies report the correlation
432 of H3K27me3 and DNA methylation at the promoters of a subset of genes [71, 73]. More
433 recently, by bisulfite sequencing of chromatin immunoprecipitated DNA, Statham et al.

has reported that H3K27me3 can co-occur with either unmethylated or methylated DNA [76]. In addition, DNA hypomethylation resulted from induced H3K27me3 reduction is observed at promoters of many genes in K27M mutant pediatric high-grade gliomas [53]. These findings indicate that change in the level of H3K27me3 at specific gene promoters affects promoter DNA methylation.

Using biochemical and MeDIP assays, we demonstrate that depletion of UTX expression by shRNAs or pharmacological inhibition of its H3K27 demethylase by GSK-J4 results in increased DNA methylation of latent HIV-1 in Jurkat T cells. DNA methylation occurs at the 5'CpG and NCR CpG clusters, surrounding the HIV-1 TSS (**Fig 5**). Similar DNA methylation patterns were seen in Th17 primary cells after treatment with GSK-J4 (**Fig 6D**). In addition, targeted next-generation bisulfite sequencing assays performed on CD4+ memory T cells isolated from well-suppressed HIV-1 infected donors also demonstrate a significant induction of DNA methylation at the 5'LTR CpG cluster when proviruses are treated with GSK-J4 (**Figs 8B & C**). The extent of DNA methylation at the HIV 5'LTR under these conditions in our study was comparable to those acquired from specific recruitment of a chimeric zinc finger DNMT1 to HIV-1 5'LTR performed in Jurkat T cells [77].

Previous reports have indicated a link between H3K27me3 and DNA methylation pathways [71, 73]. Bender et al. described that reduced H3K27me3 in K27M mutant pediatric high-grade gliomas results in DNA hypomethylation in many genes [53]. An earlier study demonstrated the correlation between DNA hypermethylation and loss of bivalent chromatin [78]. Though the precise molecular mechanisms involved have yet to be clarified, it is likely that H3K27me3 retention and H3K4me3 loss at HIV-1 5'LTR caused

by UTX depletion or GSK-J4 (**Figs 3B to 3D**) mediates the recruitment of DNA methyltransferases, including DNMT3A, to HIV-1 (**Fig 5E & F**). This hypothesis is supported by several studies showing that elevation of H3K27me3 or retention of H3K27me3 and loss of H3K4me3 is correlated with DNA hypermethylation [53, 76, 78]. Recruitment of de novo DNA methyltransferase DNMT3A to the 5'LTR CpG upon inhibition of UTX/JMJD3 by GSK-J4 likely results in induction of DNA methylation at that region; however, the involvement of DNMT1 in this process could not be refuted.

We consistently observed that the largest increase of methylation at the HIV 5'LTR occurs at CpG-1, a region that does not overlap with the majority of transcription factor binding sites. We hypothesize that methylation at this CpG-1 indirectly prevents the recruitment of transcription activators to the nearby locations by mediating recruitment of DNMTs. However, further elucidation is still required to reveal how methylation at this CpG dinucleotide negates HIV-1 transcription.

Implications for the "block and lock strategy" for a functional HIV cure

The inhibitory effect of GSK-J4 on latent HIV-1 reactivation in Jurkat T cells (**Fig 3A**), Th17 primary T cells (**Fig 6E**), and CD4+ memory T cells from HIV-1 infected donors (**Fig 7B**), demonstrates its potential as an agent for blocking HIV-1 rebound in infected patients. In addition to its inhibition of UTX, the ability of GSK-J4 to induce 5'LTR DNA methylation of latent HIV-1, although only temporary, is intriguing as it relates to "block and lock" studies of the irreversible silencing of latent HIV-1.

Among gene silencing mechanisms, DNA methylation at promoters has been suggested as a mechanism for the stable suppression of gene expression. DNA methylation at promoters is involved in imprinted X inactivation [79], and in suppression

of human endogenous retroviruses (HERVs) [80]. Unlike the heavy DNA methylation at the LTR of HERVs (more than 30% [81]), DNA methylation at 5'LTR CpG cluster of latent HIV-1 is scarcely detected in this study (the average observed DNA methylation is less than 1% - **Fig 8B**) and other studies [62-65], indicating that latent HIV-1 is actually maintained in a poised state rather than a stably repressed state like imprinted genes on inactive X chromosome or HERVs. It is unclear what determines the differences of DNA methylation observed between latent HIV-1 and HERVs. Possession of a defective genome cannot account for this variance given that only 45% of latent HIV-1 clones from patients have large deletions [65].

We hypothesize that DNA methylation at the HIV LTR is highly dynamic. Since knock out of the DNA demethylases TET1 or TET2 only partially inhibited HIV-1 reactivation in Jurkat cells (**Fig 5E**), it seems likely that the involvement of multiple TET proteins lead to rapid HIV-1 demethylation. Similarly, it is notable that GSK-J4 only temporarily promotes DNA methylation at 5'LTR of HIV-1 by recruitment of DNMT3A. A rapid turnover of DNA methylation at the HIV LTR could therefore explain the extremely low levels of DNA methylation measured at 5' LTR of latent HIV-1 in comparison to those detected at imprinted X genes or HERVs.

Our study is the first one to report that DNA methylation of latent HIV-1 can be induced by a small molecule inhibitor like GSK-J4. It is a measure of the great potency of these epigenetic restrictions that under these conditions, latency reversal due to TCR activation was blocked by over 70% in patient cells, with some donors showing nearly complete blocks to reactivation. Nonetheless, these powerful epigenetic blocks did not lead to long-term epigenetic silencing. We are therefore skeptical that the long-term HIV

503 silencing following treatment of cells by didehydro-cortistatin A is primarily due to
504 epigenetic silencing [17-20]. Alternative mechanisms could include the selective loss of
505 cells carrying proviruses during dCA exposure or reactivation, or long-term inhibition of a
506 cellular cofactor required for transcription, such as the mediator complex. These and other
507 possibilities need to be evaluated as potential explanations for these provocative
508 observations.

509 In summary, our study documents the essential role of UTX as an activator for HIV-
510 1 transcription as well as a mediator for maintaining the bivalent chromatin at the 5' LTR
511 of latent HIV-1 proviruses. We have identified GSK-J4, a H3K27 demethylase inhibitor,
512 as a potential agent for blocking latent HIV-1 reactivation in T cells. Unexpectedly, GSK-
513 J4 has been shown to be able to induce DNA methylation of latent HIV-1, but
514 unfortunately, the induction of DNA methylation by GSK-J4 on HIV-1 was only maintained
515 in the presence of GSK-J4 and could not persist after GSK-J4 removal. Methods to further
516 enhance DNA methylation at the HIV LTR should be further explored as part of a "block
517 and lock" strategy. These could include targeted recruitment of DNMTs to HIV-1 [77, 82,
518 83], and induction of DNA methylation by piRNA production [84]. However, since DNA
519 methylation by DNMT3A and DNA demethylation by TET1 and TET2 are highly dynamic,
520 it presents a formidable barrier to achieving the permanent epigenetic silencing of HIV
521 proviruses.

Materials and Methods

Cell lines and cell culture reagents

E4, 2D10, and 3C9 latently HIV-1 infected Jurkat T cell lines were used [24]. E4 and 2D10 cells were infected with Nef deleted HIV-1, while 3C9 cell line contained Nef + HIV-1. Cells were cultured in HyClone RPMI medium with L-glutamine, 5% fetal bovine serum (FBS), penicillin (100 IU/ml), streptomycin (100 µg/ml) in 5% CO_2 at 37°C. Primary T cells were cultured in RPMI medium supplemented with 10% FBS, 1 mg/ml normocin (Invivogen, ant-nr), and 25 mM HEPES pH 7.2.

VSV-G pseudotyped HIV-1 virus production

VSV-G pseudotyped HIV-1 was produced as previously described using the Thy1.2-d2EGFP-Nef-pHR' vector (which expresses Thy1.2, Nef, and d2EGFP), as well as the pdR8.91 and VSV-G vectors [24]. Cells were infected with HIV-1 by spinoculating with viruses at 3480 rpm for 1.5 hrs at room temperature.

UTX shRNA, TET1/TET2 CRISPR-Cas9, *H3.3 mutant*, and *Dnmt3a*-3xFlag constructs

Two sequences of UTX shRNAs were used: UTX-1(TGGAACAGCTCCGCGCAAATA) and UTX-2(TGCACTTGCAGCACGAATTAA). shRNAs were cloned into pLVTHM plasmid which was a gift from Didier Trono (Addgene plasmid # 12247). We replaced GFP from pLVTHM with mCherry for selection. HA tagged *H3.3* wild type (wt) and K27M lentiviral vectors were received from the previous study [52]. *H3.3* K4M and K4M-K27M mutants were made by site-directed mutagenesis from the *H3.3* wt and K27M constructs. *Dnmt3a*-3xFlag lentiviral construct was ordered from VectorBuilder (vector ID: VB180918-1067xya). Guide RNAs targeting TET1

(GCATGGAAGAGTCCTCTCTC and AAAGGCCTGTCCTAGGAAAG) or TET2 (TTCTGGGTGTAAGCTTGCCT and GGTTGATACTGAAGAATTGA) were cloned into the lentiCRISPR v2 (Addgene #52961). Lentiviral production and transduction of cells with viruses were described previously [23]

Western blot

The following antibodies were used for Western blot: UTX (A302-374A, Bethyl), β-actin (sc-47778, Santa-Cruz), Histone H3 (ab1791, Abcam), Histone H3K27me3 (ab6002, Abcam), Histone H3K4me3 (ab8580, Abcam), Histone H3K4me2 (ab1220, Abcam), HA tag (sc805, Santa-Cruz), Flag M2 (F1804, Sigma), and α-tubulin (ab4074, Abcam). Western blot was performed as described previously [24]. Fifty μg of total cell lysate per lane was loaded.

ChIP-qPCR analysis

Chromatin immunoprecipitation (ChIP) was performed as previously described using the Pierce Agarose ChIP Kit (Thermo Scientific) [23, 24]. The following antibodies were used for ChIP: RNAP II (17-672, Millipore) or (sc-899, Santa Cruz), EZH2 (17-662, Millipore), Histone H3 (ab1791, Abcam), Histone H3K4me3 (ab8580, Abcam), Histone H3K27me3 (ab6002, Abcam), and UTX antibody (A302-374A, Bethyl). The Flag M2 magnetic beads (M8823, Sigma) were used to immunoprecipitate DNMT3A-3xFlag in (Fig 6) following the same protocol for ChIP. The percentage of input method was used to calculate the enrichment of proteins at specific regions of HIV-1 genome. Primers were used for amplification of GAPDH and TNFα promoters: TNF-F: CCCCCTCGGAATCGGA, TNF-R: GAGCTCATCTGGAGGAAGCG, GAPDH-F: CGGTGCGTGCCCAGTT, GAPDH-R: CCCTACTTTCTCCCCGCTTT.

Methylated DNA immunoprecipitation (MeDIP)

DNA was isolated by Qiagen DNeasy kit, then sonicated for 20 minutes (30 second ON/30 second OFF) to generate fragments with the size of 500 bp. Two μg of DNA was heat-denatured for 10 minutes at 95°C to produce single-stranded DNA. Two μg of antibody against 5-methyl cytosine (ab10805, Abcam) was used to immunoprecipitate methylated DNA fragment for overnight. Bound DNA was washed thoroughly and eluted for quantitative measurement by qPCR. The following primers were used for qPCR: 5'LTRCpG-F: GAAGTGTTAGAGTGGAGGTTTGA, 5'LTRCpG-R: CAGCGGAAAGTCCCTTGTAG, EnvCpG-F: TTTGTTCCTTGGGTTCTTGG, EnvCpG-R: TGGTGCAAATGAGTTTTCCA.

Production of HIV-1 latently infected primary cells and virus reactivation

HIV-1 latently infected Th17 primary cells (QUECEL) were produced following previously described procedure [61] and using Thy1.2-d2EGFP-Nef-pHR' construct. Reactivation of proviruses was performed by incubating cells overnight with Dynabeads® Human T-Activator CD3/CD28 (25 μl/10^6 cells) or a combination of SAHA (1 μM) and IL15 (10 ng/ml).

Treatment of E4 cell line with 5'-Azacytidine (5-AZC)

5-AZC was purchased from Sigma (A2385) and dissolved in 50% acetic acid. Cells were pretreated with 1 μM 5-AZC for 72 hours then left untreated or treated further with a combination of anti-CD3 (125 ng/ml) and anti-CD28 (500 ng/ml), 500 nM of SAHA, or 1 ng/ml of TNFα overnight. HIV-1 reactivation in the cells was measured by FACS. Fold of HIV-1 reactivation was calculated by normalizing the levels of d2EGFP expression after drugs treatment to those obtained from the 5-AZC untreated conditions.

Treatment of HIV-1 latently infected Jurkat cells and primary cells with inhibitors

GSK-J4 was purchased from Selleckchem (S7070) and dissolved in DMSO. Cells were treated with increasing concentrations of GSK-J4. Cell viability was measured by propidium iodide (5 µg/ml, 10008351-Cayman) or calcein AM viability dye (65-0854-39-eBioscience) staining.

RNA induction assay (EDITS assay)

CD4+ memory T cells isolated from HIV-1 infected donors were treated with GSK-J4 for 3 days. Then cells were stimulated overnight with Dynabeads® Human T-Activator CD3/CD28, followed by staining with anti-CD69 (1:100 dilution, 557745 –BD Pharmingen) and FACS analysis. EDITS assays to measure the reactivation of latent HIV-1 in CD4+ memory T cells isolated from well suppressed HIV-1 infected donors were performed as described previously [61].

Targeted next-generation bisulfite sequencing

PBMCs were purified from fresh blood samples, which were collected following the guidelines from an approved IRB protocol, using Ficoll-Paque. CD4+ memory T cells were isolated by human memory CD4 T cell enrichment kit (19157, Stemcell). Cells were cultured as a million cells per ml in RPMI media supplemented with 10% FBS and 15 units/ml of IL2. Cells were treated with 0 or 5 μM of GSK-J4 for 72 hours. Total genomic DNA was isolated using DNeasy Blood & Tissue Kit (69504, Qiagen). Bisulfite conversion of DNA was performed by EZ DNA methylation-lightning kit (D5030, Zymo research) using 1.5 μg of DNA per reaction. Nested PCR to amplify the 5' LTR CpG cluster of HIV-1 was performed as described previously [56] using 125 ng of bisulfite-treated DNA per reaction. Ion torrent A and P1 sequencing adapters and barcode sequences were

614 incorporated to the primers used for the second round of PCR by oligo synthesis. The
615 amplified PCR products were gel purified and loaded on the ion 540 or 520 Chip for next-
616 generation sequencing using the Ion Chef and Ion S5 sequencing system (ThermoFisher)
617 following manufacturer's protocol. CpG methylation was analyzed by QUMA with the
618 default settings [85] using the 5'LTR sequence from the HBX2 strain as reference.
619

620 ## Acknowledgment

621 We thank Robert Assad and Miguel E. Quiñones-Mateu for providing us blood
622 samples from HIV-1 infected donors. We also thank former and present members of the
623 Karn laboratory and Nga Le for help and useful discussion. This work was supported by
624 US Public Health Service grants R01 MH110360, R01 DA043159, R01 AI148083 and
625 amfAR grant 109347-59-RGRL to JK. We also thank the CWRU/UH Center for AIDS
626 Research (P30-AI036219) for provision of flow cytometry services.

627

References

1. Davey RT, Jr., Bhat N, Yoder C, Chun TW, Metcalf JA, Dewar R, et al. HIV-1 and T cell dynamics after interruption of highly active antiretroviral therapy (HAART) in patients with a history of sustained viral suppression. Proc Natl Acad Sci U S A. 1999;96(26):15109-14. PubMed PMID: 10611346; PubMed Central PMCID: PMCPMC24781.

2. Zhang L, Chung C, Hu BS, He T, Guo Y, Kim AJ, et al. Genetic characterization of rebounding HIV-1 after cessation of highly active antiretroviral therapy. J Clin Invest. 2000;106(7):839-45. doi: 10.1172/JCI10565. PubMed PMID: 11018071; PubMed Central PMCID: PMCPMC517816.

3. Kim Y, Anderson JL, Lewin SR. Getting the "Kill" into "Shock and Kill": Strategies to Eliminate Latent HIV. Cell Host Microbe. 2018;23(1):14-26. doi: 10.1016/j.chom.2017.12.004. PubMed PMID: 29324227.

4. Yeh YJ, Ho YC. Shock-and-kill versus block-and-lock: Targeting the fluctuating and heterogeneous HIV-1 gene expression. Proc Natl Acad Sci U S A. 2021;118(16). Epub 2021/03/25. doi: 10.1073/pnas.2103692118. PubMed PMID: 33758027.

5. Li JZ, Gandhi RT. The Search for an HIV Cure: Where Do We Go From Here? J Infect Dis. 2021;223(Supplement_1):1-3. Epub 2021/02/16. doi: 10.1093/infdis/jiaa738. PubMed PMID: 33586774; PubMed Central PMCID: PMCPMC7883020.

6. Siliciano JD, Siliciano RF. Low Inducibility of Latent Human Immunodeficiency Virus Type 1 Proviruses as a Major Barrier to Cure. J Infect Dis.

649 2021;223(Supplement_1):13-21. Epub 2021/02/16. doi: 10.1093/infdis/jiaa649. PubMed
650 PMID: 33586775; PubMed Central PMCID: PMCPMC7883034.

651 7. Pache L, Marsden MD, Teriete P, Portillo AJ, Heimann D, Kim JT, et al.
652 Pharmacological Activation of Non-canonical NF-κB Signaling Activates Latent HIV-1
653 Reservoirs In Vivo. Cell Rep Med. 2020;1(3):100037. Epub 2020/11/19. doi:
654 10.1016/j.xcrm.2020.100037. PubMed PMID: 33205060; PubMed Central PMCID:
655 PMCPMC7659604.

656 8. Ait-Ammar A, Kula A, Darcis G, Verdikt R, De Wit S, Gautier V, et al. Current Status
657 of Latency Reversing Agents Facing the Heterogeneity of HIV-1 Cellular and Tissue
658 Reservoirs. Front Microbiol. 2019;10:3060. Epub 2020/02/11. doi:
659 10.3389/fmicb.2019.03060. PubMed PMID: 32038533; PubMed Central PMCID:
660 PMCPMC6993040.

661 9. Lichterfeld M. Reactivation of latent HIV moves shock-and-kill treatments forward.
662 Nature. 2020;578(7793):42-3. Epub 2020/02/06. doi: 10.1038/d41586-020-00010-x.
663 PubMed PMID: 32020104.

664 10. McMahon DK, Zheng L, Cyktor JC, Aga E, Macatangay BJ, Godfrey C, et al. A
665 phase I/II randomized, placebo-controlled trial of romidepsin in persons with HIV-1 on
666 suppressive antiretroviral therapy to assess safety and activation of HIV-1 expression
667 (A5315). J Infect Dis. 2020. Epub 2020/12/23. doi: 10.1093/infdis/jiaa777. PubMed PMID:
668 33349862.

669 11. Gunst JD, Højen JF, Søgaard OS. Broadly neutralizing antibodies combined with
670 latency-reversing agents or immune modulators as strategy for HIV-1 remission. Curr
671 Opin HIV AIDS. 2020;15(5):309-15. Epub 2020/07/18. doi:
672 10.1097/coh.0000000000000641. PubMed PMID: 32675575.

673 12. Herzig E, Kim KC, Packard TA, Vardi N, Schwarzer R, Gramatica A, et al. Attacking
674 Latent HIV with convertibleCAR-T Cells, a Highly Adaptable Killing Platform. Cell.
675 2019;179(4):880-94.e10. Epub 2019/11/02. doi: 10.1016/j.cell.2019.10.002. PubMed
676 PMID: 31668804; PubMed Central PMCID: PMCPMC6922308.

677 13. Powell AB, Ren Y, Korom M, Saunders D, Hanley PJ, Goldstein H, et al.
678 Engineered Antigen-Specific T Cells Secreting Broadly Neutralizing Antibodies:
679 Combining Innate and Adaptive Immune Response against HIV. Mol Ther Methods Clin
680 Dev. 2020;19:78-88. Epub 2020/10/03. doi: 10.1016/j.omtm.2020.08.015. PubMed PMID:
681 33005704; PubMed Central PMCID: PMCPMC7508916.

682 14. Kessing CF, Nixon CC, Li C, Tsai P, Takata H, Mousseau G, et al. In Vivo
683 Suppression of HIV Rebound by Didehydro-Cortistatin A, a "Block-and-Lock" Strategy for
684 HIV-1 Treatment. Cell Rep. 2017;21(3):600-11. doi: 10.1016/j.celrep.2017.09.080.
685 PubMed PMID: 29045830; PubMed Central PMCID: PMCPMC5653276.

686 15. Vansant G, Bruggemans A, Janssens J, Debyser Z. Block-And-Lock Strategies to
687 Cure HIV Infection. Viruses. 2020;12(1). Epub 2020/01/16. doi: 10.3390/v12010084.
688 PubMed PMID: 31936859; PubMed Central PMCID: PMCPMC7019976.

16. Ahlenstiel CL, Symonds G, Kent SJ, Kelleher AD. Block and Lock HIV Cure Strategies to Control the Latent Reservoir. Front Cell Infect Microbiol. 2020;10:424. Epub 2020/09/15. doi: 10.3389/fcimb.2020.00424. PubMed PMID: 32923412; PubMed Central PMCID: PMCPMC7457024.

17. Li C, Mori L, Valente ST. The Block-and-Lock Strategy for Human Immunodeficiency Virus Cure: Lessons Learned from Didehydro-Cortistatin A. J Infect Dis. 2021;223(Supplement_1):46-53. Epub 2021/02/16. doi: 10.1093/infdis/jiaa681. PubMed PMID: 33586776; PubMed Central PMCID: PMCPMC7883021.

18. Li C, Mousseau G, Valente ST. Tat inhibition by didehydro-Cortistatin A promotes heterochromatin formation at the HIV-1 long terminal repeat. Epigenetics Chromatin. 2019;12(1):23. Epub 2019/04/18. doi: 10.1186/s13072-019-0267-8. PubMed PMID: 30992052; PubMed Central PMCID: PMCPMC6466689.

19. Kessing CF, Nixon CC, Li C, Tsai P, Takata H, Mousseau G, et al. In Vivo Suppression of HIV Rebound by Didehydro-Cortistatin A, a "Block-and-Lock" Strategy for HIV-1 Treatment. Cell Rep. 2017;21(3):600-11. Epub 2017/10/19. doi: 10.1016/j.celrep.2017.09.080. PubMed PMID: 29045830; PubMed Central PMCID: PMCPMC5653276.

20. Mousseau G, Kessing CF, Fromentin R, Trautmann L, Chomont N, Valente ST. The Tat Inhibitor Didehydro-Cortistatin A Prevents HIV-1 Reactivation from Latency. MBio. 2015;6(4):e00465. Epub 2015/07/15. doi: 10.1128/mBio.00465-15. PubMed PMID: 26152583; PubMed Central PMCID: PMCPMC4495168.

710 21. Mbonye U, Karn J. The Molecular Basis for Human Immunodeficiency Virus
711 Latency. Annu Rev Virol. 2017;4(1):261-85. doi: 10.1146/annurev-virology-101416-
712 041646. PubMed PMID: 28715973.

713 22. Dobrowolski C, Valadkhan S, Graham AC, Shukla M, Ciuffi A, Telenti A, et al. Entry
714 of Polarized Effector Cells into Quiescence Forces HIV Latency. MBio. 2019;10(2). Epub
715 2019/03/28. doi: 10.1128/mBio.00337-19. PubMed PMID: 30914509.

716 23. Nguyen K, Das B, Dobrowolski C, Karn J. Multiple Histone Lysine
717 Methyltransferases Are Required for the Establishment and Maintenance of HIV-1
718 Latency. MBio. 2017;8(1). doi: 10.1128/mBio.00133-17. PubMed PMID: 28246360;
719 PubMed Central PMCID: PMCPMC5347344.

720 24. Friedman J, Cho WK, Chu CK, Keedy KS, Archin NM, Margolis DM, et al.
721 Epigenetic silencing of HIV-1 by the histone H3 lysine 27 methyltransferase enhancer of
722 Zeste 2. J Virol. 2011;85(17):9078-89. doi: 10.1128/JVI.00836-11. PubMed PMID:
723 21715480; PubMed Central PMCID: PMCPMC3165831.

724 25. Olson A, Basukala B, Lee S, Gagne M, Wong WW, Henderson AJ. Targeted
725 Chromatinization and Repression of HIV-1 Provirus Transcription with Repurposed
726 CRISPR/Cas9. Viruses. 2020;12(10). Epub 2020/10/16. doi: 10.3390/v12101154.
727 PubMed PMID: 33053801; PubMed Central PMCID: PMCPMC7600714.

728 26. Boehm D, Ott M. Host Methyltransferases and Demethylases: Potential New
729 Epigenetic Targets for HIV Cure Strategies and Beyond. AIDS Res Hum Retroviruses.

730 2017;33(S1):S8-s22. Epub 2017/11/16. doi: 10.1089/aid.2017.0180. PubMed PMID:
731 29140109; PubMed Central PMCID: PMCPMC5684665.

732 27. Boehm D, Jeng M, Camus G, Gramatica A, Schwarzer R, Johnson JR, et al.
733 SMYD2-Mediated Histone Methylation Contributes to HIV-1 Latency. Cell Host Microbe.
734 2017;21(5):569-79 e6. doi: 10.1016/j.chom.2017.04.011. PubMed PMID: 28494238;
735 PubMed Central PMCID: PMCPMC5490666.

736 28. Kumar A, Darcis G, Van Lint C, Herbein G. Epigenetic control of HIV-1 post
737 integration latency: implications for therapy. Clinical epigenetics. 2015;7:103. Epub
738 2015/09/26. doi: 10.1186/s13148-015-0137-6. PubMed PMID: 26405463; PubMed
739 Central PMCID: PMCPMC4581042.

740 29. Tyagi M, Pearson RJ, Karn J. Establishment of HIV latency in primary CD4+ cells
741 is due to epigenetic transcriptional silencing and P-TEFb restriction. J Virol.
742 2010;84(13):6425-37. doi: 10.1128/JVI.01519-09. PubMed PMID: 20410271; PubMed
743 Central PMCID: PMCPMC2903277.

744 30. Turner AW, Dronamraju R, Potjewyd F, James KS, Winecoff DK, Kirchherr JL, et
745 al. Evaluation of EED Inhibitors as a Class of PRC2-Targeted Small Molecules for HIV
746 Latency Reversal. ACS Infect Dis. 2020;6(7):1719-33. Epub 2020/04/30. doi:
747 10.1021/acsinfecdis.9b00514. PubMed PMID: 32347704; PubMed Central PMCID:
748 PMCPMC7359025.

749 31. Krasnopolsky S, Kuzmina A, Taube R. Genome-wide CRISPR knockout screen
750 identifies ZNF304 as a silencer of HIV transcription that promotes viral latency. PLoS

751 Pathog. 2020;16(9):e1008834. Epub 2020/09/22. doi: 10.1371/journal.ppat.1008834.
752 PubMed PMID: 32956422; PubMed Central PMCID: PMCPMC7529202.

753 32. Lindqvist B, Svensson Akusjärvi S, Sönnerborg A, Dimitriou M, Svensson JP.
754 Chromatin maturation of the HIV-1 provirus in primary resting CD4+ T cells. PLoS Pathog.
755 2020;16(1):e1008264. Epub 2020/01/31. doi: 10.1371/journal.ppat.1008264. PubMed
756 PMID: 31999790; PubMed Central PMCID: PMCPMC6991963.

757 33. Zapata JC, Campilongo F, Barclay RA, DeMarino C, Iglesias-Ussel MD, Kashanchi
758 F, et al. The Human Immunodeficiency Virus 1 ASP RNA promotes viral latency by
759 recruiting the Polycomb Repressor Complex 2 and promoting nucleosome assembly.
760 Virology. 2017;506:34-44. Epub 2017/03/25. doi: 10.1016/j.virol.2017.03.002. PubMed
761 PMID: 28340355; PubMed Central PMCID: PMCPMC5505171.

762 34. Swigut T, Wysocka J. H3K27 demethylases, at long last. Cell. 2007;131(1):29-32.
763 doi: 10.1016/j.cell.2007.09.026. PubMed PMID: 17923085.

764 35. Agger K, Cloos PA, Christensen J, Pasini D, Rose S, Rappsilber J, et al. UTX and
765 JMJD3 are histone H3K27 demethylases involved in HOX gene regulation and
766 development. Nature. 2007;449(7163):731-4. doi: 10.1038/nature06145. PubMed PMID:
767 17713478.

768 36. Dhar SS, Lee SH, Chen K, Zhu G, Oh W, Allton K, et al. An essential role for UTX
769 in resolution and activation of bivalent promoters. Nucleic Acids Res. 2016;44(8):3659-
770 74. doi: 10.1093/nar/gkv1516. PubMed PMID: 26762983; PubMed Central PMCID:
771 PMCPMC4856969.

772 37. Taube JH, Sphyris N, Johnson KS, Reisenauer KN, Nesbit TA, Joseph R, et al.
773 The H3K27me3-demethylase KDM6A is suppressed in breast cancer stem-like cells, and
774 enables the resolution of bivalency during the mesenchymal-epithelial transition.
775 Oncotarget. 2017;8(39):65548-65. doi: 10.18632/oncotarget.19214. PubMed PMID:
776 29029452; PubMed Central PMCID: PMCPMC5630352.

777 38. Moore LD, Le T, Fan G. DNA methylation and its basic function.
778 Neuropsychopharmacology. 2013;38(1):23-38.

779 39. Xie W, Barr CL, Kim A, Yue F, Lee AY, Eubanks J, et al. Base-resolution analyses
780 of sequence and parent-of-origin dependent DNA methylation in the mouse genome. Cell.
781 2012;148(4):816-31.

782 40. Achour M, Jacq X, Ronde P, Alhosin M, Charlot C, Chataigneau T, et al. The
783 interaction of the SRA domain of ICBP90 with a novel domain of DNMT1 is involved in
784 the regulation of VEGF gene expression. Oncogene. 2008;27(15):2187-97. doi:
785 10.1038/sj.onc.1210855. PubMed PMID: 17934516.

786 41. Lopes EC, Valls E, Figueroa ME, Mazur A, Meng FG, Chiosis G, et al. Kaiso
787 contributes to DNA methylation-dependent silencing of tumor suppressor genes in colon
788 cancer cell lines. Cancer Res. 2008;68(18):7258-63. doi: 10.1158/0008-5472.CAN-08-
789 0344. PubMed PMID: 18794111.

790 42. Jones PA. Functions of DNA methylation: islands, start sites, gene bodies and
791 beyond. Nat Rev Genet. 2012;13(7):484-92. doi: 10.1038/nrg3230. PubMed PMID:
792 22641018.

793 43. Blazkova J, Trejbalova K, Gondois-Rey F, Halfon P, Philibert P, Guiguen A, et al.
794 CpG methylation controls reactivation of HIV from latency. PLoS Pathog.
795 2009;5(8):e1000554. PubMed PMID: 19696893.

796 44. Kauder SE, Bosque A, Lindqvist A, Planelles V, Verdin E. Epigenetic regulation of
797 HIV-1 latency by cytosine methylation. PLoS Pathog. 2009;5(6):e1000495. PubMed
798 PMID: 19557157.

799 45. Blazkova J, Murray D, Justement JS, Funk EK, Nelson A, Moir S, et al. Paucity of
800 HIV DNA Methylation in Latently Infected, Resting CD4+ T Cells from Infected Individuals
801 Receiving Antiretroviral Therapy. J Virol. 2012;86(9):5390-2. Epub 2012/02/22. doi:
802 10.1128/JVI.00040-12. PubMed PMID: 22345448.

803 46. Palacios JA, Perez-Pinar T, Toro C, Sanz-Minguela B, Moreno V, Valencia E, et
804 al. Long-term nonprogressor and elite controller patients who control viremia have a
805 higher percentage of methylation in their HIV-1 proviral promoters than aviremic patients
806 receiving highly active antiretroviral therapy. J Virol. 2012;86(23):13081-4. Epub
807 2012/09/14. doi: 10.1128/JVI.01741-12. PubMed PMID: 22973038; PubMed Central
808 PMCID: PMC3497688.

809 47. Pearson R, Kim YK, Hokello J, Lassen K, Friedman J, Tyagi M, et al. Epigenetic
810 silencing of human immunodeficiency virus (HIV) transcription by formation of restrictive
811 chromatin structures at the viral long terminal repeat drives the progressive entry of HIV
812 into latency. J Virol. 2008;82(24):12291-303. PubMed PMID: 18829756.

813 48. Zhang HS, Du GY, Liu Y, Zhang ZG, Zhou Z, Li H, et al. UTX-1 regulates Tat-
814 induced HIV-1 transactivation via changing the methylated status of histone H3. Int J
815 Biochem Cell Biol. 2016;80:51-6. doi: 10.1016/j.biocel.2016.09.016. PubMed PMID:
816 27671333.

817 49. Jadlowsky JK, Wong JY, Graham AC, Dobrowolski C, Devor RL, Adams MD, et
818 al. Negative elongation factor is required for the maintenance of proviral latency but does
819 not induce promoter-proximal pausing of RNA polymerase II on the HIV long terminal
820 repeat. Mol Cell Biol. 2014;34(11):1911-28. doi: 10.1128/MCB.01013-13. PubMed PMID:
821 24636995; PubMed Central PMCID: PMCPMC4019061.

822 50. Voigt P, Tee WW, Reinberg D. A double take on bivalent promoters. Genes Dev.
823 2013;27(12):1318-38. doi: 10.1101/gad.219626.113. PubMed PMID: 23788621; PubMed
824 Central PMCID: PMCPMC3701188.

825 51. Blanco E, Gonzalez-Ramirez M, Alcaine-Colet A, Aranda S, Di Croce L. The
826 Bivalent Genome: Characterization, Structure, and Regulation. Trends Genet.
827 2020;36(2):118-31. Epub 2019/12/11. doi: 10.1016/j.tig.2019.11.004. PubMed PMID:
828 31818514.

829 52. Lewis PW, Muller MM, Koletsky MS, Cordero F, Lin S, Banaszynski LA, et al.
830 Inhibition of PRC2 activity by a gain-of-function H3 mutation found in pediatric
831 glioblastoma. Science. 2013;340(6134):857-61. doi: 10.1126/science.1232245. PubMed
832 PMID: 23539183; PubMed Central PMCID: PMCPMC3951439.

833 53. Bender S, Tang Y, Lindroth AM, Hovestadt V, Jones DT, Kool M, et al. Reduced
834 H3K27me3 and DNA hypomethylation are major drivers of gene expression in K27M
835 mutant pediatric high-grade gliomas. Cancer Cell. 2013;24(5):660-72. doi:
836 10.1016/j.ccr.2013.10.006. PubMed PMID: 24183680.

837 54. Fontebasso AM, Papillon-Cavanagh S, Schwartzentruber J, Nikbakht H, Gerges
838 N, Fiset PO, et al. Recurrent somatic mutations in ACVR1 in pediatric midline high-grade
839 astrocytoma. Nat Genet. 2014;46(5):462-6. doi: 10.1038/ng.2950. PubMed PMID:
840 24705250; PubMed Central PMCID: PMCPMC4282994.

841 55. Sturm D, Witt H, Hovestadt V, Khuong-Quang DA, Jones DT, Konermann C, et al.
842 Hotspot mutations in H3F3A and IDH1 define distinct epigenetic and biological subgroups
843 of glioblastoma. Cancer Cell. 2012;22(4):425-37. doi: 10.1016/j.ccr.2012.08.024.
844 PubMed PMID: 23079654.

845 56. Trejbalova K, Kovarova D, Blazkova J, Machala L, Jilich D, Weber J, et al.
846 Development of 5' LTR DNA methylation of latent HIV-1 provirus in cell line models and
847 in long-term-infected individuals. Clin Epigenetics. 2016;8:19. doi: 10.1186/s13148-016-
848 0185-6. PubMed PMID: 26900410; PubMed Central PMCID: PMCPMC4759744.

849 57. Leung DC, Dong KB, Maksakova IA, Goyal P, Appanah R, Lee S, et al. Lysine
850 methyltransferase G9a is required for de novo DNA methylation and the establishment,
851 but not the maintenance, of proviral silencing. Proc Natl Acad Sci U S A.
852 2011;108(14):5718-23. Epub 2011/03/24. doi: 10.1073/pnas.1014660108. PubMed
853 PMID: 21427230; PubMed Central PMCID: PMC3078371.

854 58. Pion M, Jordan A, Biancotto A, Dequiedt F, Gondois-Rey F, Rondeau S, et al.
855 Transcriptional suppression of in vitro-integrated human immunodeficiency virus type 1
856 does not correlate with proviral DNA methylation. J Virol. 2003;77:4025-32.

857 59. Stresemann C, Lyko F. Modes of action of the DNA methyltransferase inhibitors
858 azacytidine and decitabine. Int J Cancer. 2008;123(1):8-13. doi: 10.1002/ijc.23607.
859 PubMed PMID: 18425818.

860 60. Chavez L, Kauder S, Verdin E. In vivo, in vitro, and in silico analysis of methylation
861 of the HIV-1 provirus. Methods. 2011;53(1):47-53. doi: 10.1016/j.ymeth.2010.05.009.
862 PubMed PMID: 20670606; PubMed Central PMCID: PMCPMC3566233.

863 61. Das B, Dobrowolski C, Luttge B, Valadkhan S, Chomont N, Johnston R, et al.
864 Estrogen receptor-1 is a key regulator of HIV-1 latency that imparts gender-specific
865 restrictions on the latent reservoir. Proc Natl Acad Sci U S A. 2018;115(33):E7795-E804.
866 doi: 10.1073/pnas.1803468115. PubMed PMID: 30061382; PubMed Central PMCID:
867 PMCPMC6099847.

868 62. Blazkova J, Murray D, Justement JS, Funk EK, Nelson AK, Moir S, et al. Paucity
869 of HIV DNA methylation in latently infected, resting CD4+ T cells from infected individuals
870 receiving antiretroviral therapy. J Virol. 2012;86(9):5390-2. doi: 10.1128/JVI.00040-12.
871 PubMed PMID: 22345448; PubMed Central PMCID: PMCPMC3347337.

872 63. Palacios JA, Perez-Pinar T, Toro C, Sanz-Minguela B, Moreno V, Valencia E, et
873 al. Long-term nonprogressor and elite controller patients who control viremia have a
874 higher percentage of methylation in their HIV-1 proviral promoters than aviremic patients

receiving highly active antiretroviral therapy. J Virol. 2012;86(23):13081-4. doi: 10.1128/JVI.01741-12. PubMed PMID: 22973038; PubMed Central PMCID: PMCPMC3497688.

64. Weber S, Weiser B, Kemal KS, Burger H, Ramirez CM, Korn K, et al. Epigenetic analysis of HIV-1 proviral genomes from infected individuals: predominance of unmethylated CpG's. Virology. 2014;449:181-9. doi: 10.1016/j.virol.2013.11.013. PubMed PMID: 24418551; PubMed Central PMCID: PMCPMC4060985.

65. Ho YC, Shan L, Hosmane NN, Wang J, Laskey SB, Rosenbloom DI, et al. Replication-competent noninduced proviruses in the latent reservoir increase barrier to HIV-1 cure. Cell. 2013;155(3):540-51. doi: 10.1016/j.cell.2013.09.020. PubMed PMID: 24243014; PubMed Central PMCID: PMCPMC3896327.

66. Issaeva I, Zonis Y, Rozovskaia T, Orlovsky K, Croce CM, Nakamura T, et al. Knockdown of ALR (MLL2) reveals ALR target genes and leads to alterations in cell adhesion and growth. Mol Cell Biol. 2007;27(5):1889-903. doi: 10.1128/MCB.01506-06. PubMed PMID: 17178841; PubMed Central PMCID: PMCPMC1820476.

67. Kimpton J, Emerman M. Detection of replication-competent and pseudotyped human immunodeficiency virus with a sensitive cell line on the basis of activation of an integrated beta-galactosidase gene. J Virol. 1992;66(4):2232-9. PubMed PMID: 1548759; PubMed Central PMCID: PMCPMC289016.

894 68. Bernstein BE, Mikkelsen TS, Xie X, Kamal M, Huebert DJ, Cuff J, et al. A bivalent
895 chromatin structure marks key developmental genes in embryonic stem cells. Cell.
896 2006;125(2):315-26. doi: 10.1016/j.cell.2006.02.041. PubMed PMID: 16630819.

897 69. Mikkelsen TS, Ku M, Jaffe DB, Issac B, Lieberman E, Giannoukos G, et al.
898 Genome-wide maps of chromatin state in pluripotent and lineage-committed cells. Nature.
899 2007;448(7153):553-60. doi: 10.1038/nature06008. PubMed PMID: 17603471; PubMed
900 Central PMCID: PMCPMC2921165.

901 70. Kauder SE, Bosque A, Lindqvist A, Planelles V, Verdin E. Epigenetic regulation of
902 HIV-1 latency by cytosine methylation. PLoS Pathog. 2009;5(6):e1000495. doi:
903 10.1371/journal.ppat.1000495. PubMed PMID: 19557157; PubMed Central PMCID:
904 PMCPMC2695767.

905 71. Meissner A, Mikkelsen TS, Gu H, Wernig M, Hanna J, Sivachenko A, et al.
906 Genome-scale DNA methylation maps of pluripotent and differentiated cells. Nature.
907 2008;454(7205):766-70. doi: 10.1038/nature07107. PubMed PMID: 18600261; PubMed
908 Central PMCID: PMCPMC2896277.

909 72. Brunner AL, Johnson DS, Kim SW, Valouev A, Reddy TE, Neff NF, et al. Distinct
910 DNA methylation patterns characterize differentiated human embryonic stem cells and
911 developing human fetal liver. Genome Res. 2009;19(6):1044-56. doi:
912 10.1101/gr.088773.108. PubMed PMID: 19273619; PubMed Central PMCID:
913 PMCPMC2694474.

914 73. Gal-Yam EN, Egger G, Iniguez L, Holster H, Einarsson S, Zhang X, et al. Frequent
915 switching of Polycomb repressive marks and DNA hypermethylation in the PC3 prostate
916 cancer cell line. Proc Natl Acad Sci U S A. 2008;105(35):12979-84. doi:
917 10.1073/pnas.0806437105. PubMed PMID: 18753622; PubMed Central PMCID:
918 PMCPMC2529074.

919 74. Takeshima H, Yamashita S, Shimazu T, Niwa T, Ushijima T. The presence of RNA
920 polymerase II, active or stalled, predicts epigenetic fate of promoter CpG islands.
921 Genome Res. 2009;19(11):1974-82. doi: 10.1101/gr.093310.109. PubMed PMID:
922 19652013; PubMed Central PMCID: PMCPMC2775588.

923 75. Hahn MA, Hahn T, Lee DH, Esworthy RS, Kim BW, Riggs AD, et al. Methylation
924 of polycomb target genes in intestinal cancer is mediated by inflammation. Cancer Res.
925 2008;68(24):10280-9. doi: 10.1158/0008-5472.CAN-08-1957. PubMed PMID: 19074896;
926 PubMed Central PMCID: PMCPMC2491345.

927 76. Statham AL, Robinson MD, Song JZ, Coolen MW, Stirzaker C, Clark SJ. Bisulfite
928 sequencing of chromatin immunoprecipitated DNA (BisChIP-seq) directly informs
929 methylation status of histone-modified DNA. Genome Res. 2012;22(6):1120-7. doi:
930 10.1101/gr.132076.111. PubMed PMID: 22466171; PubMed Central PMCID:
931 PMCPMC3371705.

932 77. Deng J, Qu X, Lu P, Yang X, Zhu Y, Ji H, et al. Specific and Stable Suppression
933 of HIV Provirus Expression In Vitro by Chimeric Zinc Finger DNA Methyltransferase 1.
934 Mol Ther Nucleic Acids. 2017;6:233-42. doi: 10.1016/j.omtn.2017.01.002. PubMed PMID:
935 28325289; PubMed Central PMCID: PMCPMC5363508.

936 78. Bernhart SH, Kretzmer H, Holdt LM, Juhling F, Ammerpohl O, Bergmann AK, et
937 al. Changes of bivalent chromatin coincide with increased expression of developmental
938 genes in cancer. Sci Rep. 2016;6:37393. doi: 10.1038/srep37393. PubMed PMID:
939 27876760; PubMed Central PMCID: PMCPMC5120258.

940 79. Cotton AM, Price EM, Jones MJ, Balaton BP, Kobor MS, Brown CJ. Landscape of
941 DNA methylation on the X chromosome reflects CpG density, functional chromatin state
942 and X-chromosome inactivation. Hum Mol Genet. 2015;24(6):1528-39. doi:
943 10.1093/hmg/ddu564. PubMed PMID: 25381334; PubMed Central PMCID:
944 PMCPMC4381753.

945 80. Hurst TP, Magiorkinis G. Epigenetic Control of Human Endogenous Retrovirus
946 Expression: Focus on Regulation of Long-Terminal Repeats (LTRs). Viruses. 2017;9(6).
947 doi: 10.3390/v9060130. PubMed PMID: 28561791; PubMed Central PMCID:
948 PMCPMC5490807.

949 81. Lavie L, Kitova M, Maldener E, Meese E, Mayer J. CpG methylation directly
950 regulates transcriptional activity of the human endogenous retrovirus family HERV-
951 K(HML-2). J Virol. 2005;79(2):876-83. doi: 10.1128/JVI.79.2.876-883.2005. PubMed
952 PMID: 15613316; PubMed Central PMCID: PMCPMC538560.

953 82. Pflueger C, Tan D, Swain T, Nguyen T, Pflueger J, Nefzger C, et al. A modular
954 dCas9-SunTag DNMT3A epigenome editing system overcomes pervasive off-target
955 activity of direct fusion dCas9-DNMT3A constructs. Genome Res. 2018;28(8):1193-206.
956 doi: 10.1101/gr.233049.117. PubMed PMID: 29907613; PubMed Central PMCID:
957 PMCPMC6071642.

958 83. Martinez-Colom A, Lasarte S, Fernandez-Pineda A, Relloso M, Munoz-Fernandez
959 MA. A new chimeric protein represses HIV-1 LTR-mediated expression by DNA
960 methylase. Antiviral Res. 2013;98(3):394-400. doi: 10.1016/j.antiviral.2013.04.007.
961 PubMed PMID: 23588231.

962 84. Itou D, Shiromoto Y, Yukiho SY, Ishii C, Nishimura T, Ogonuki N, et al. Induction
963 of DNA methylation by artificial piRNA production in male germ cells. Curr Biol.
964 2015;25(7):901-6. doi: 10.1016/j.cub.2015.01.060. PubMed PMID: 25772451.

965 85. Kumaki Y, Oda M, Okano M. QUMA: quantification tool for methylation analysis.
966 Nucleic Acids Res. 2008;36(Web Server issue):W170-5. doi: 10.1093/nar/gkn294.
967 PubMed PMID: 18487274; PubMed Central PMCID: PMCPMC2447804.
968

Figure legends

Fig 1. Inhibition of HIV-1 reactivation in UTX knocked down E4 cells.

(A) Representative FACS measuring d2EGFP expression in two UTX knocked down clones from E4 cells stimulated with TNFα (10 ng/ml) overnight. (B) Quantification of HIV-1 reactivation in two clones from UTX knocked down E4 cells, UTX knocked down 2D10, and UTX knocked down 3C9 cells stimulated with indicated conditions. 3C9 cells habors Nef+, Wt Tat HIV, while 2D10 cells are infected with H13L mutant Tat HIV-1. Error bars: SEM of 3 separate experiments. (C) d2EGFP expression in UTX knocked down E4 clones left untreated or stimulated with SAHA (2 μM) overnight. Two tailed, Mann Whitney test was used for statistical calculation. (D) Western blot measuring the levels of UTX and H3K27me3 in E4 cells expressing scramble or UTX shRNAs.

Fig 2. UTX functions as a transcription activator of HIV-1 transcription.

ChIP assays measuring the enrichments of (A) RNAPII, (B) UTX, (C) EZH2 and (D) H3K27me3 at the nuc0, HIV-1 promoter, and nuc1 regions of latent or reactivated HIV-1. Latent proviruses in E4 cells were reactivated by TNFα (10 ng/ml) for an hour. ChIP assays measuring the enrichment of (E) RNAPII and (F) UTX along HIV-1 genome in one UTX knocked down clone. Error bars: SEM of 3 separate quantitative real-time PCRs.

Fig 3. Inhibition of UTX demethylase activity by GSK-J4 prevents HIV-1 reactivation in Jurkat T cells.

(A) Quantification of d2EGFP expression in E4 and 3C9 cells pretreated with increasing concentrations of GSK-J4 for 24 hours and stimulated with SAHA (2 μM) or TNFα (10 ng/ml) overnight. Error bars: SEM of 5 separate experiments. One-way ANOVA, $P < 0.05$, Bonferroni posttests * $p < 0.05$, ** $p<0.01$, *** $p<0.001$, n=5. ChIP assays measuring the

enrichments of (B) RNAPII, (C) H3K4me3 and (D) H3K27me3 at the 5'LTR of HIV-1 when latent proviruses were left unstimulated or reactivated for an hour by TNFα (10 ng/ml) with or without the presence of GSK-J4 (10 μM). E4 cells were pretreated for 24 hours with GSK-J4 (10 μM) then further stimulated with TNFα (10 ng/ml) for an hour. Error bars: SEM of 3 separate quantitative real-time PCRs.

Fig 4. H3K4 methylation is crucial for HIV-1 reactivation mediated by H3K27 removal.

(A) Western blot measuring the indicated histone H3 methylation levels of cells expressing HA tagged wild type (wt) H3.3 or indicated mutants of H3.3. The upper bands (marked with *) from blots with antibodies against H3K27me3 and H3 are from the H3.3-HA variants (B) Quantification of HIV-1 reactivation in E4 cells expressing wt H3.3 or indicated H3.3 mutants. Presented statistical significance was based on comparison with H3.3 K27M variant. One-way ANOVA, n=5 $p<0.005$, Bonferroni posttests, * $p<0.05$,** $p<0.01$, *** $p<0.001$. Error bars: SEM of 5 different replications.

Fig 5. Depletion of UTX elevates DNA methylation levels of latent HIV-1 in Jurkat T cells due to enhanced recruitment of DNMT3A to HIV-1 5'LTR

(A) The map indicates the positions of CpG islands and primer binding sites along HIV-1 genome. (B) HIV-1 reactivation in UTX knocked down cells treated with 5-AZC. E4 cells were pretreated with 1 μM 5-AZC for 72 hours then left untreated or treated further with a combination of anti-CD3 (125 ng/ml) and anti-CD28 (500 ng/ml), 500 nM of SAHA, or 1 ng/ml of TNFα overnight. HIV-1 reactivation in the cells was measured by FACS. Error bars: SEM of at least 3 separate replicates. T-test, n=3 * $p < 0.05$. (C) MeDIP assay measuring the levels of methylated cytosine of HIV-1 in UTX knock down E4 cells or E4

cells treated with 10 μM of GSK-J4 for 48 hours. Error bars: SEM of 3 separate quantitative real-time PCRs. (D) Expression levels of DNMT3A in E4 cells transduced with lentiviruses harboring *Dnmt3a*-3xFlag and ChIP assays performed on cells treated with indicated conditions using Flag MS2 magnetic beads to pull down DNMT3A-3xFlag proteins. Cells were transduced and selected by puromycin (2 μg/ml) for 3 days. Before ChIP, cells were treated with GSK-J4 for 48 hours. Error bars: SEM of 3 separate quantitative real-time PCRs. (E) DNA demethylases TET1 and TET2 are involved in HIV-1 reactivation in Jurkat T cells. Reactivation of latent HIV-1 induced overnight by SAHA (1 μM) or TNFα (10 ng/ml) in TET1 or TET2 knocked-out E4 cells. Error bars: SEM of 3 separate triplicates. One-way ANOVA, $p < 0.05$ Bonferroni posttests, n=3 * $p < 0.05$.

Fig 6. Inhibition of UTX by GSK-J4 promotes the silencing of HIV-1 in Th17 primary cells and elevates HIV-1 DNA methylation.

(A) Schematic of experimental design. (B) Relative levels of H3K27me3 compared to histone H3 levels quantified from Western blot on treated Th17 cells from 4 donors at Day 4. One-tailed, paired t-test, * $p<0.05$. (C) Silencing kinetics of HIV-1 in Th17 cells from 4 different donors in the presence of 0 μM (vehicle) or 1 μM of GSK-J4. Error bars: SEM of at least 3 separate biological replicates. Two-way ANOVA, Bonferroni posttests, * $p<0.05$ ** $p<0.01$. (D) MeDIP measuring the levels of methylated cytosine of HIV-1 at Day 4. Error bars: SEM of 4 different donors. One-tailed, paired t-test, n=4, * $p<0.05$. (E) GSK-J4 inhibits the reactivation of latent HIV-1 by SAHA & IL15 or TCR stimulation in Th17 primary cells. Cells were pretreated for 48 hours with GSK-J4, then further stimulated overnight with SAHA & IL15 or Human T-Activator CD3/CD28 Dynabeads with the ratio of 25 μl of beads per 1 million cells. Quantification of HIV-1 reactivation under the

indicated conditions. Error bars: SEM of 3 separate triplicates. One-way ANOVA, Bonferroni posttests n >3.

Fig 7. GSK-J4 inhibits reactivation of latent HIV-1 in CD4 memory T cells isolated from well suppressed HIV-1 infected donors.

(A) Schematic diagrams describing the experimental designs. (B) Inhibition of latent HIV-1 reactivation in CD4+ memory T cells from HIV-1 infected patients on HAARTs by UTX inhibitor. CD4+ memory T cells isolated from HIV-1 infected patients were treated for 3 days with indicated concentrations of GSK-J4. Cells were left untreated or further treated with human T-Activator CD3/CD28 Dynabeads overnight. Levels of spliced HIV-1 env mRNA were measured by EDITS assays. Levels of relative reactivation were normalized to the levels of spliced HIV-1 env mRNA induced by human T-Activator CD3/CD28 Dynabeads (presented as 100%) for each donor. (C) Expression levels of CD69 from treated CD4+ memory T cells measured by FACS using CD69 antibody. One-way ANOVA $p < 0.005$, Bonferroni posttests * $p<0.05$ ** $p<0.01$ *** $p<0.001$ was performed for both Figure 7B & 7C. (D) Intracellular H3K27me3 levels of treated CD4+ memory T cells measured by FACS using a H3K27me3 antibody. Cells were stained with Alexa Fluor 647-conjugated trimethyl histone H3 (Lys27) antibody (12158, Cell Signaling) and analyzed by FACS as described previously [23]. (E) Viability of cells by PI staining. After drug treatment, cells were stained with PI at the final concentration of 5 μg/ml for 5 minutes, then analyzed by FACS. Two-tailed paired t-test was performed for both Figure 7D & 7E, * $p<0.05$, ns: not statistically significant.

Fig 8. Temporary induction of DNA methylation at 5'LTR of latent HIV-1 in CD4 memory T cells upon the inhibition of UTX by GSK-J4

(A) The map of CpG dinucleotides (numbered from 1 to 9) relative to HIV-1 transcription start site along the 5'LTR CpG cluster. (B) The average DNA methylation (as %) of CpGs and the percentage DNA methylation at CpG island 1 of the 5'LTR CpG cluster from CD4+ memory T cells treated with the indicated concentration of GSK-J4. (C) The average DNA methylation of CpGs and the percentage DNA methylation at the CpG island 1 at the 5'LTR CpG cluster of HIV-1 from CD4+ memory T cells induced with GSK-J4 before or after GSK-J4 removal. Experiments were performed on 3 different donors. One-tailed paired t-tests were performed on all experiments, * $p<0.05$, ns: not statistically significant. Note: different HIV-1 donors were utilized for this experiment than those utilized in Figure 8B.

Supporting Information

S1 Fig. Flow cytometry assay for latency reversal in E4 cells.

Representative FACS measuring d2EGFP expression in E4 cells are shown for cells were pretreated with increasing concentrations of GSK-J4 for 24 hours and stimulated with SAHA (2 μM) or TNFα (10 ng/ml) overnight.

S2 Fig. GSK-J4 inhibits the reactivation of latent HIV-1 by SAHA & IL15 or TCR stimulation in Th17 primary cells.

(A) Experimental design. (B) Flow cytometry measuring the reactivation of HIV-1 in Th17 cells by the combination of SAHA (1 μM) and IL15 (10 ng/ml) or Human T-Activator CD3/CD28 Dynabeads in the presence of increasing concentrations of GSK-J4. Cells were pretreated for 48 hours with GSK-J4, then further stimulated overnight with SAHA & IL15 or Human T-Activator CD3/CD28 Dynabeads with the ratio of 25 μl of beads per 1 million cells.

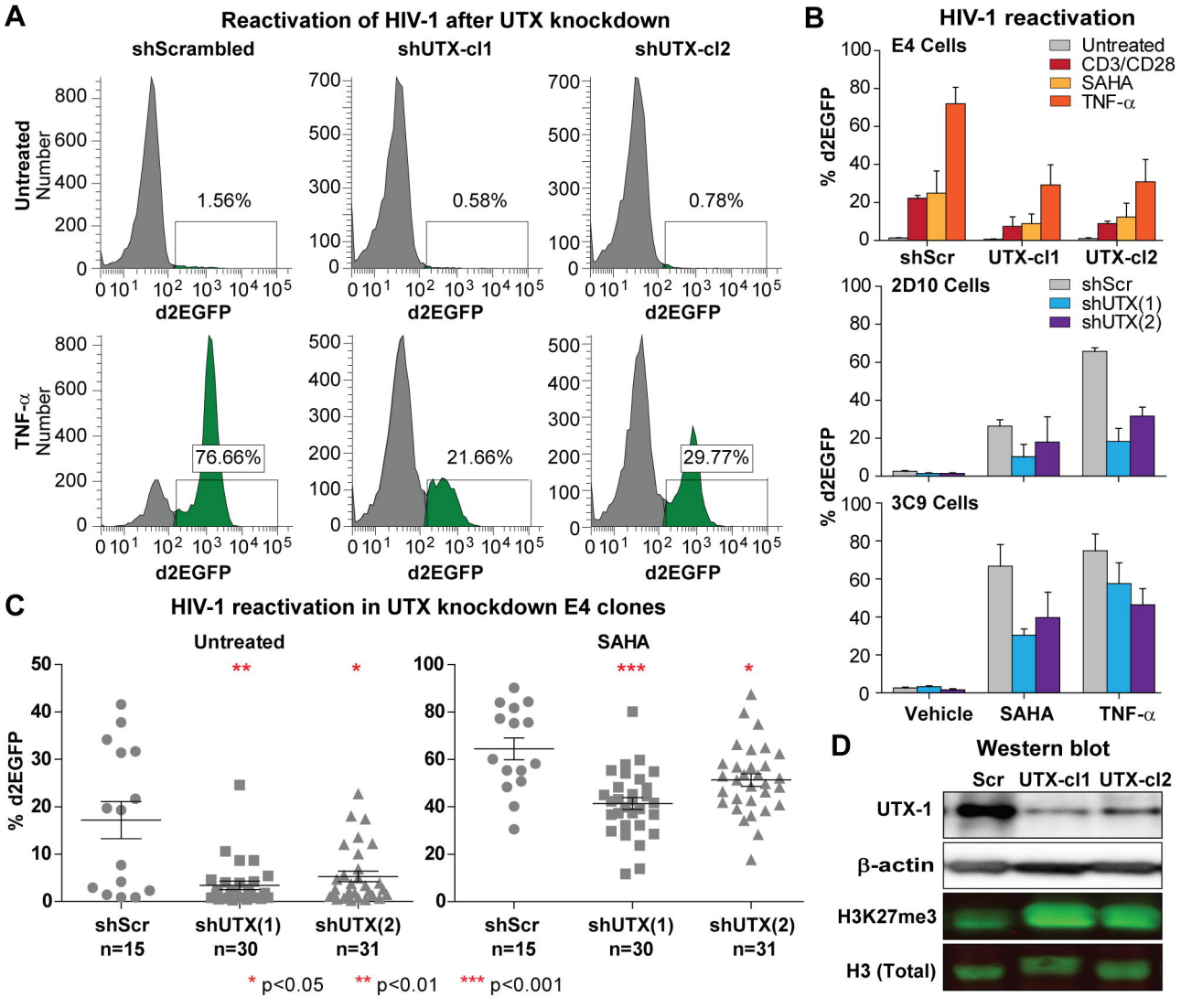
A
Reactivation of HIV-1 after UTX knockdown
shScrambled
shUTX-cl1
shUTX-cl2
Untreated
Number
TNF-α
Number
1.56%
0.58%
0.78%
76.66%
21.66%
29.77%
d2EGFP
B
HIV-1 reactivation
E4 Cells
Untreated
CD3/CD28
SAHA
TNF-α
% d2EGFP
shScr
UTX-cl1
UTX-cl2
2D10 Cells
shScr
shUTX(1)
shUTX(2)
3C9 Cells
Vehicle
SAHA
TNF-α
C
HIV-1 reactivation in UTX knockdown E4 clones
Untreated
SAHA
% d2EGFP
shScr
n=15
shUTX(1)
n=30
shUTX(2)
n=31
* p<0.05
** p<0.01
*** p<0.001
D
Western blot
Scr
UTX-cl1
UTX-cl2
UTX-1
β-actin
H3K27me3
H3 (Total)

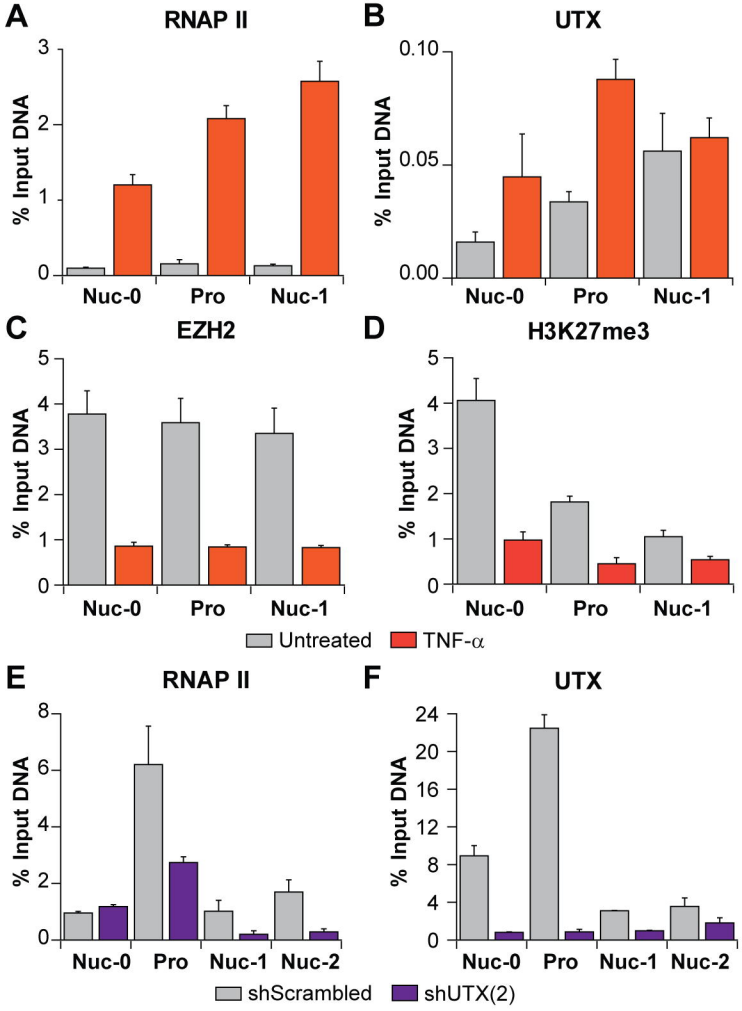
A
RNAP II
% Input DNA
3
2
1
0
Nuc-0
Pro
Nuc-1
B
UTX
% Input DNA
0.10
0.05
0.00
Nuc-0
Pro
Nuc-1
C
EZH2
% Input DNA
5
4
3
2
1
0
Nuc-0
Pro
Nuc-1
D
H3K27me3
% Input DNA
5
4
3
2
1
0
Nuc-0
Pro
Nuc-1
Untreated
TNF-α
E
RNAP II
% Input DNA
8
6
4
2
0
Nuc-0
Pro
Nuc-1
Nuc-2
F
UTX
% Input DNA
24
20
16
12
8
4
0
Nuc-0
Pro
Nuc-1
Nuc-2
shScrambled
shUTX(2)

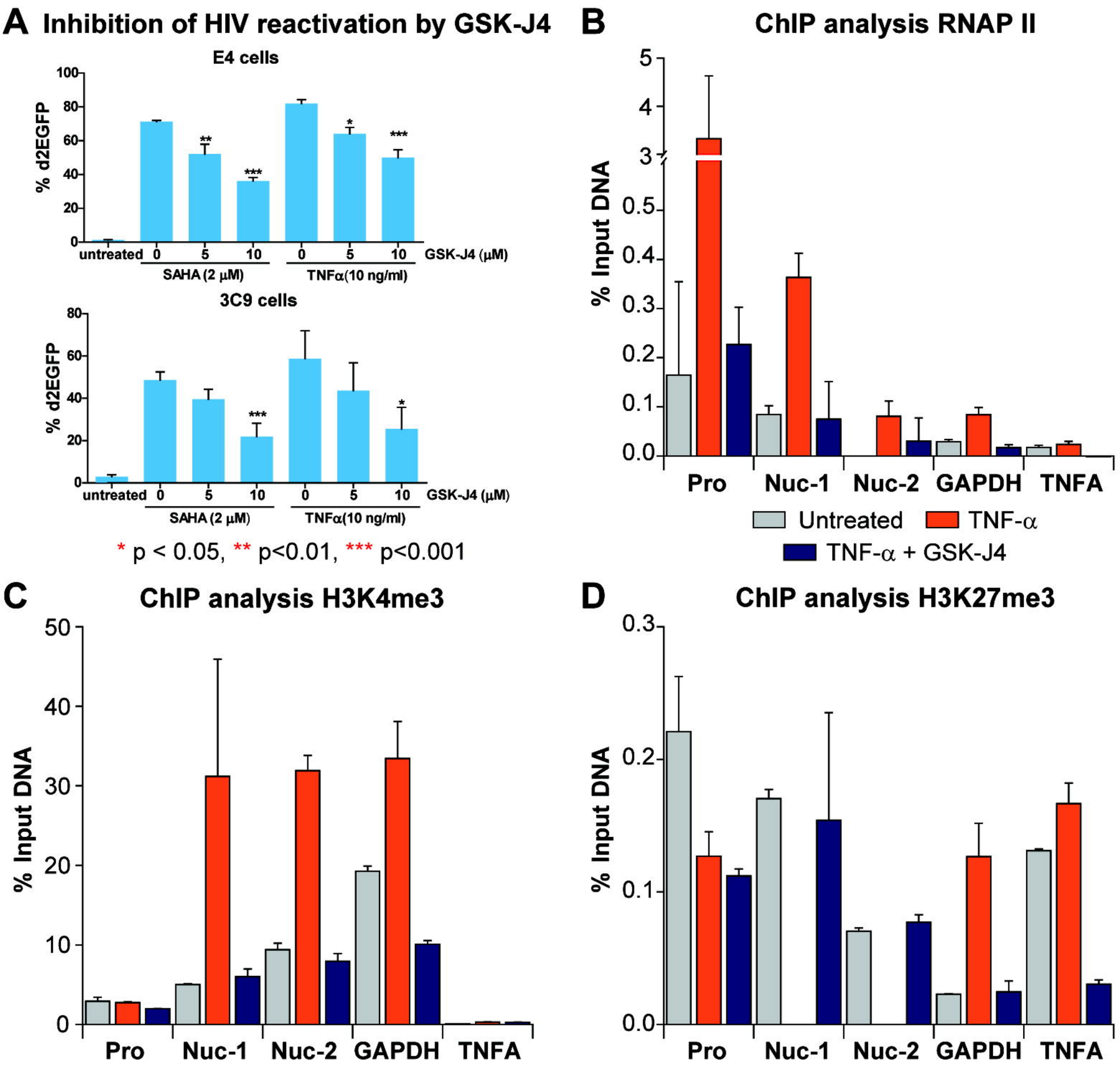
A
Inhibition of HIV reactivation by GSK-J4
E4 cells
% d2EGFP
untreated
SAHA (2 μM)
TNFα(10 ng/ml)
GSK-J4 (μM)
3C9 cells
* p < 0.05, ** p<0.01, *** p<0.001
B
ChIP analysis RNAP II
% Input DNA
Pro
Nuc-1
Nuc-2
GAPDH
TNFA
Untreated
TNF-α
TNF-α + GSK-J4
C
ChIP analysis H3K4me3
D
ChIP analysis H3K27me3

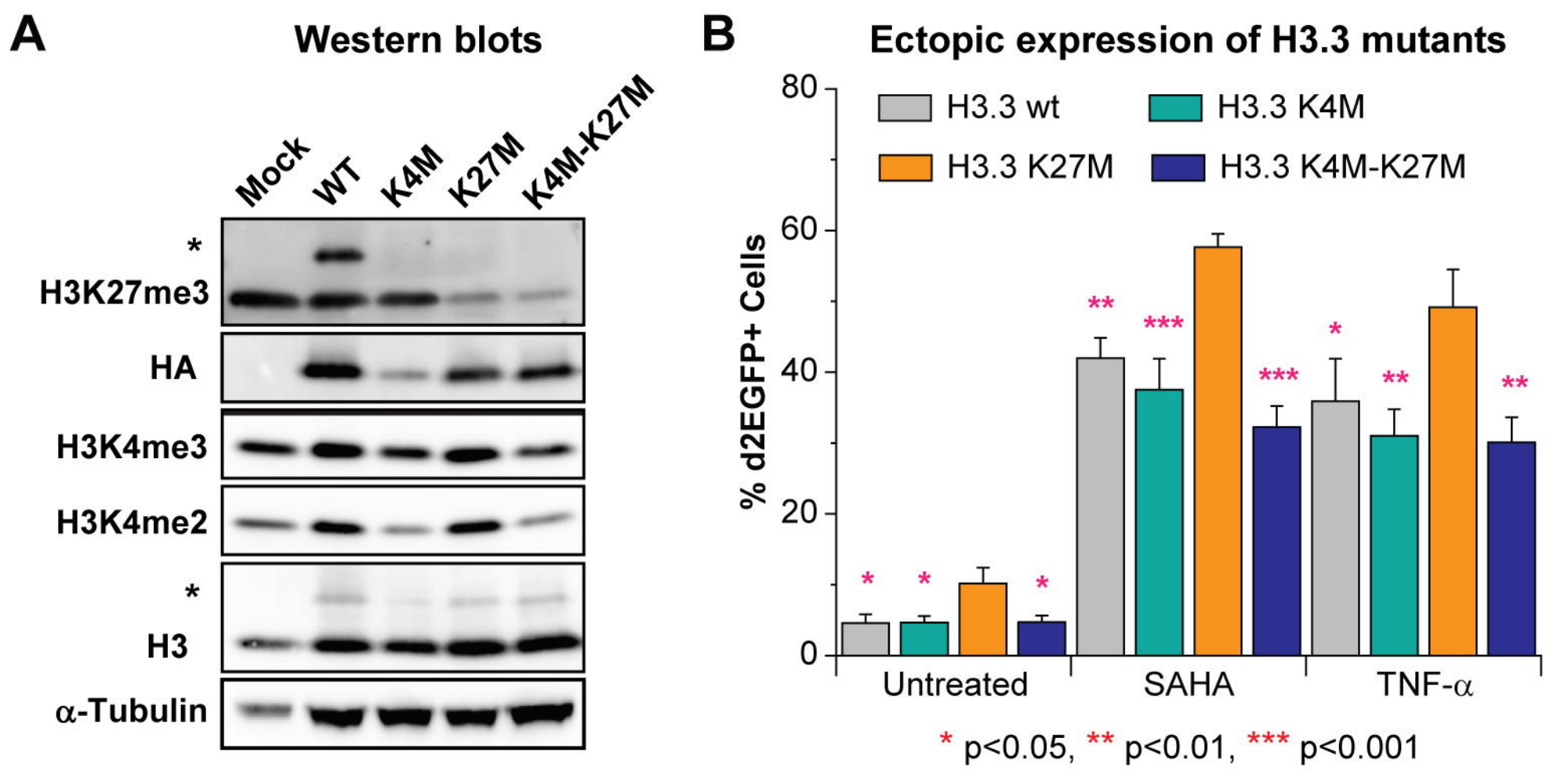
A
Western blots
Mock
WT
K4M
K27M
K4M-K27M
*
H3K27me3
HA
H3K4me3
H3K4me2
*
H3
α-Tubulin
B
Ectopic expression of H3.3 mutants
H3.3 wt
H3.3 K4M
H3.3 K27M
H3.3 K4M-K27M
% d2EGFP+ Cells
80
60
40
20
0
Untreated
SAHA
TNF-α
* p<0.05, ** p<0.01, *** p<0.001

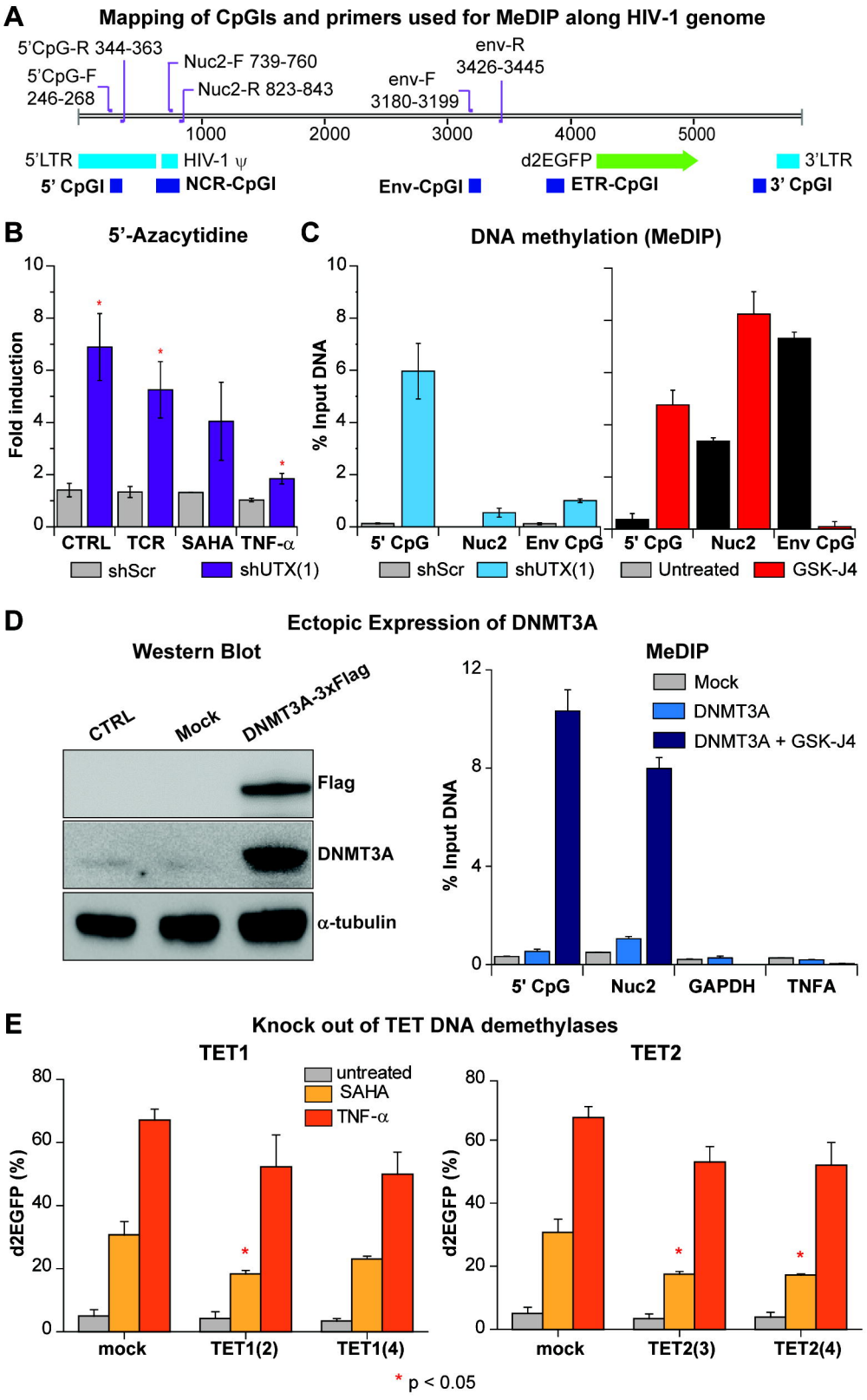
A
Mapping of CpGIs and primers used for MeDIP along HIV-1 genome
5'CpG-R 344-363
5'CpG-F 246-268
Nuc2-F 739-760
Nuc2-R 823-843
env-F 3180-3199
env-R 3426-3445
1000
2000
3000
4000
5000
5'LTR
HIV-1 ψ
d2EGFP
3'LTR
5' CpGI
NCR-CpGI
Env-CpGI
ETR-CpGI
3' CpGI
B
5'-Azacytidine
Fold induction
CTRL
TCR
SAHA
TNF-α
shScr
shUTX(1)
C
DNA methylation (MeDIP)
% Input DNA
5' CpG
Nuc2
Env CpG
shScr
shUTX(1)
Untreated
GSK-J4
D
Ectopic Expression of DNMT3A
Western Blot
CTRL
Mock
DNMT3A-3xFlag
Flag
DNMT3A
α-tubulin
MeDIP
Mock
DNMT3A
DNMT3A + GSK-J4
% Input DNA
5' CpG
Nuc2
GAPDH
TNFA
E
Knock out of TET DNA demethylases
TET1
TET2
untreated
SAHA
TNF-α
d2EGFP (%)
mock
TET1(2)
TET1(4)
TET2(3)
TET2(4)
* p < 0.05

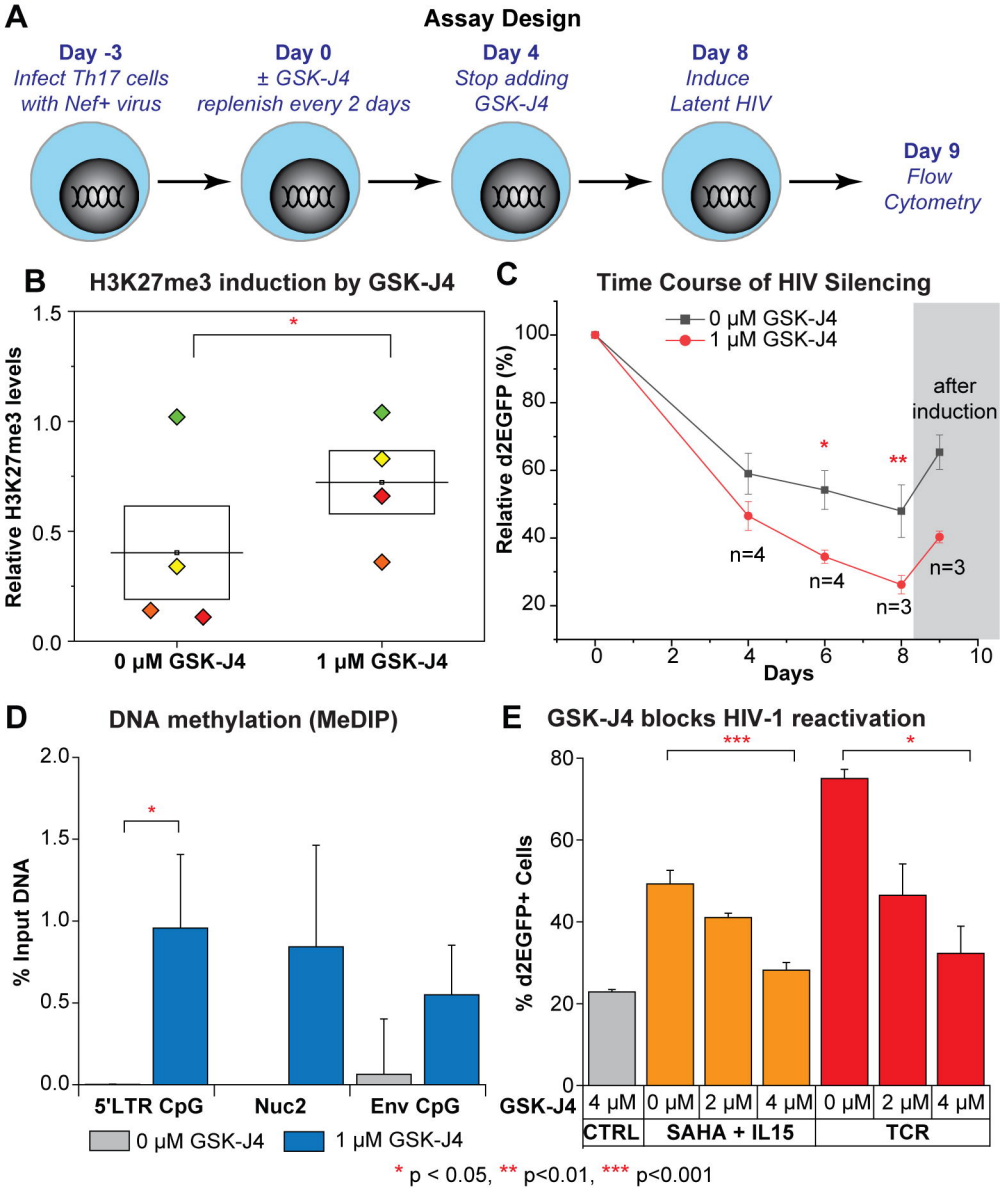
A
Assay Design
Day -3
Infect Th17 cells with Nef+ virus
Day 0
± GSK-J4 replenish every 2 days
Day 4
Stop adding GSK-J4
Day 8
Induce Latent HIV
Day 9
Flow Cytometry
B
H3K27me3 induction by GSK-J4
Relative H3K27me3 levels
1.5
1.0
0.5
0.0
*
0 μM GSK-J4
1 μM GSK-J4
C
Time Course of HIV Silencing
0 μM GSK-J4
1 μM GSK-J4
Relative d2EGFP (%)
100
80
60
40
20
after induction
*
**
n=4
n=4
n=3
n=3
0
2
4
6
8
10
Days
D
DNA methylation (MeDIP)
% Input DNA
2.0
1.5
1.0
0.5
0.0
*
5'LTR CpG
Nuc2
Env CpG
0 μM GSK-J4
1 μM GSK-J4
E
GSK-J4 blocks HIV-1 reactivation
% d2EGFP+ Cells
80
60
40
20
0
***
*
GSK-J4
4 μM
0 μM
2 μM
4 μM
0 μM
2 μM
4 μM
CTRL
SAHA + IL15
TCR
* p < 0.05, ** p<0.01, *** p<0.001

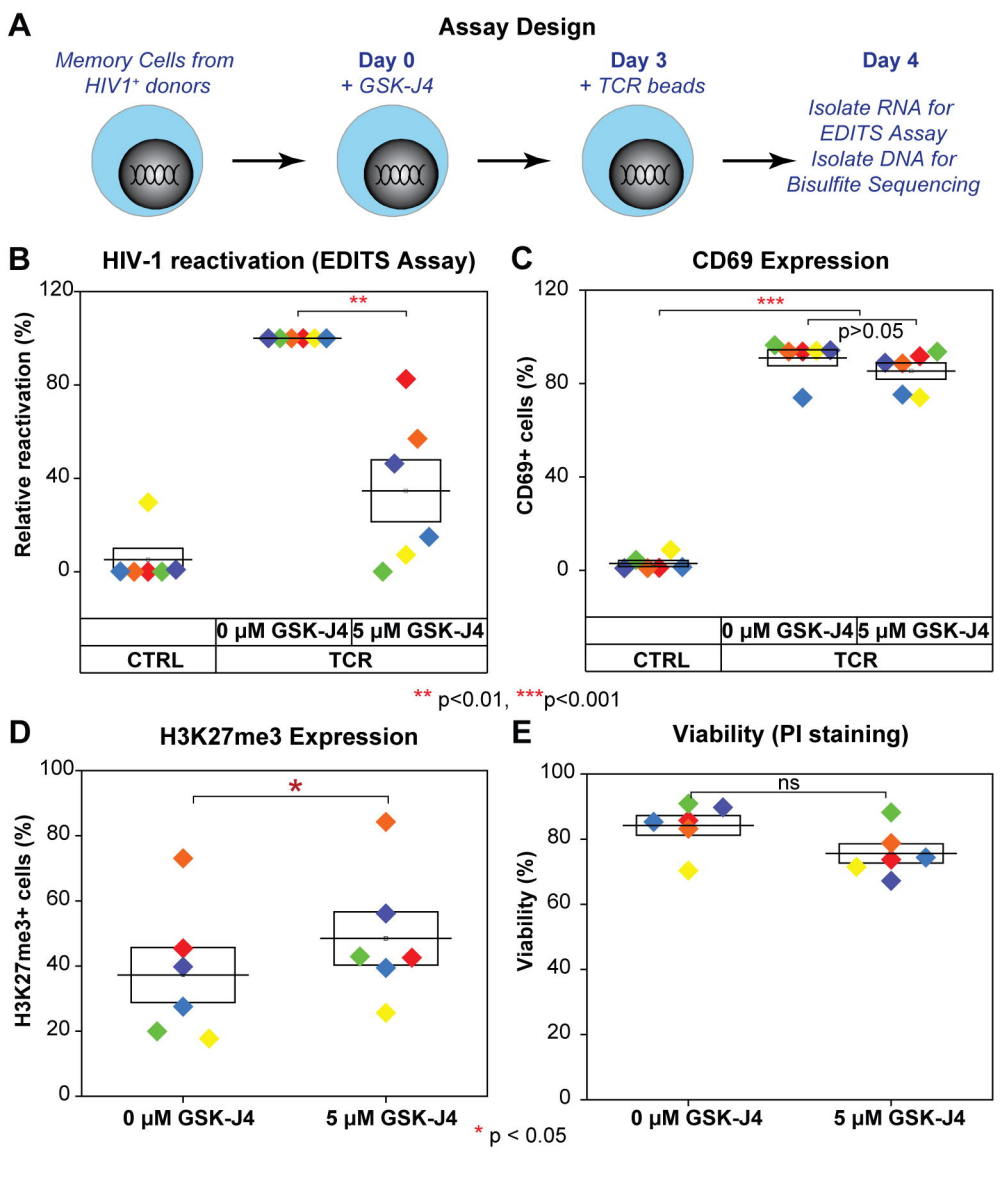
A
Assay Design
Memory Cells from HIV1+ donors
Day 0
+ GSK-J4
Day 3
+ TCR beads
Day 4
Isolate RNA for EDITS Assay
Isolate DNA for Bisulfite Sequencing
B
HIV-1 reactivation (EDITS Assay)
Relative reactivation (%)
120
80
40
0
**
0 µM GSK-J4
5 µM GSK-J4
CTRL
TCR
C
CD69 Expression
CD69+ cells (%)
120
80
40
0
***
p>0.05
0 µM GSK-J4
5 µM GSK-J4
CTRL
TCR
** p<0.01, ***p<0.001
D
H3K27me3 Expression
H3K27me3+ cells (%)
100
80
60
40
20
0
*
0 µM GSK-J4
5 µM GSK-J4
E
Viability (PI staining)
Viability (%)
100
80
60
40
20
0
ns
0 µM GSK-J4
5 µM GSK-J4
* p < 0.05

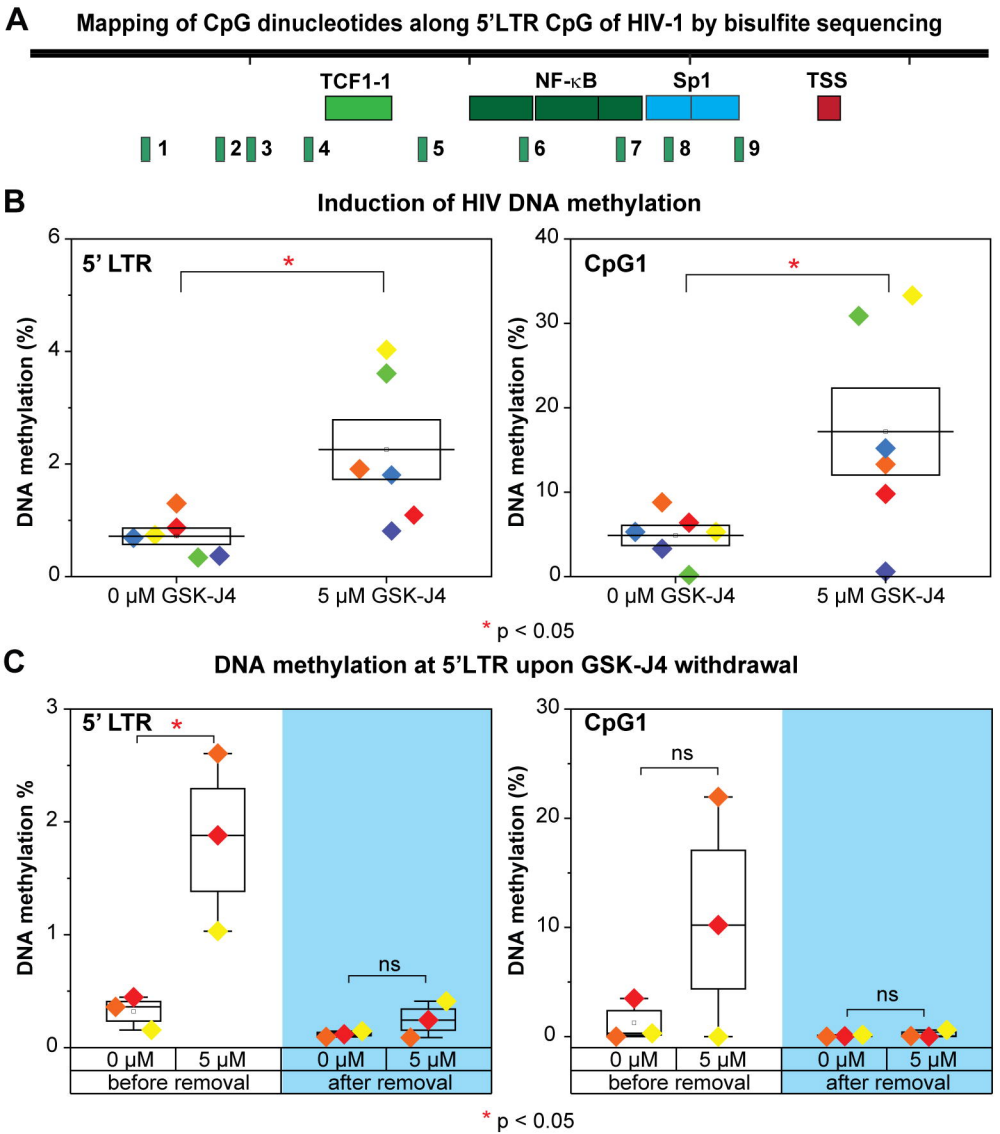
A
Mapping of CpG dinucleotides along 5'LTR CpG of HIV-1 by bisulfite sequencing
TCF1-1
NF-κB
Sp1
TSS
1
2
3
4
5
6
7
8
9
B
Induction of HIV DNA methylation
5' LTR
DNA methylation (%)
0 μM GSK-J4
5 μM GSK-J4
CpG1
* p < 0.05
C
DNA methylation at 5'LTR upon GSK-J4 withdrawal
DNA methylation %
ns
0 μM
5 μM
before removal
after removal

Inhibition of UTX1 demethylase activity by GSK-J4 prevents HIV-1 reactivation in Jurkat T cells

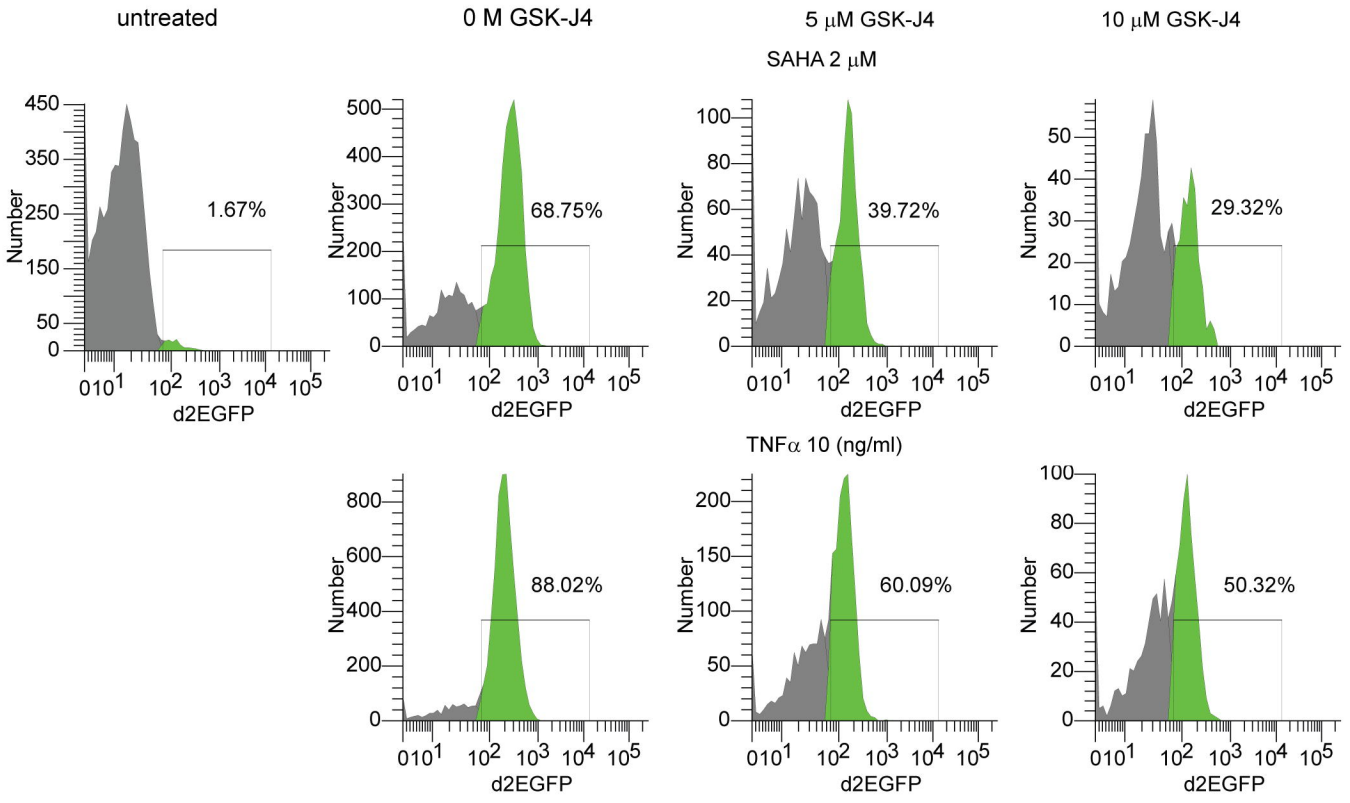

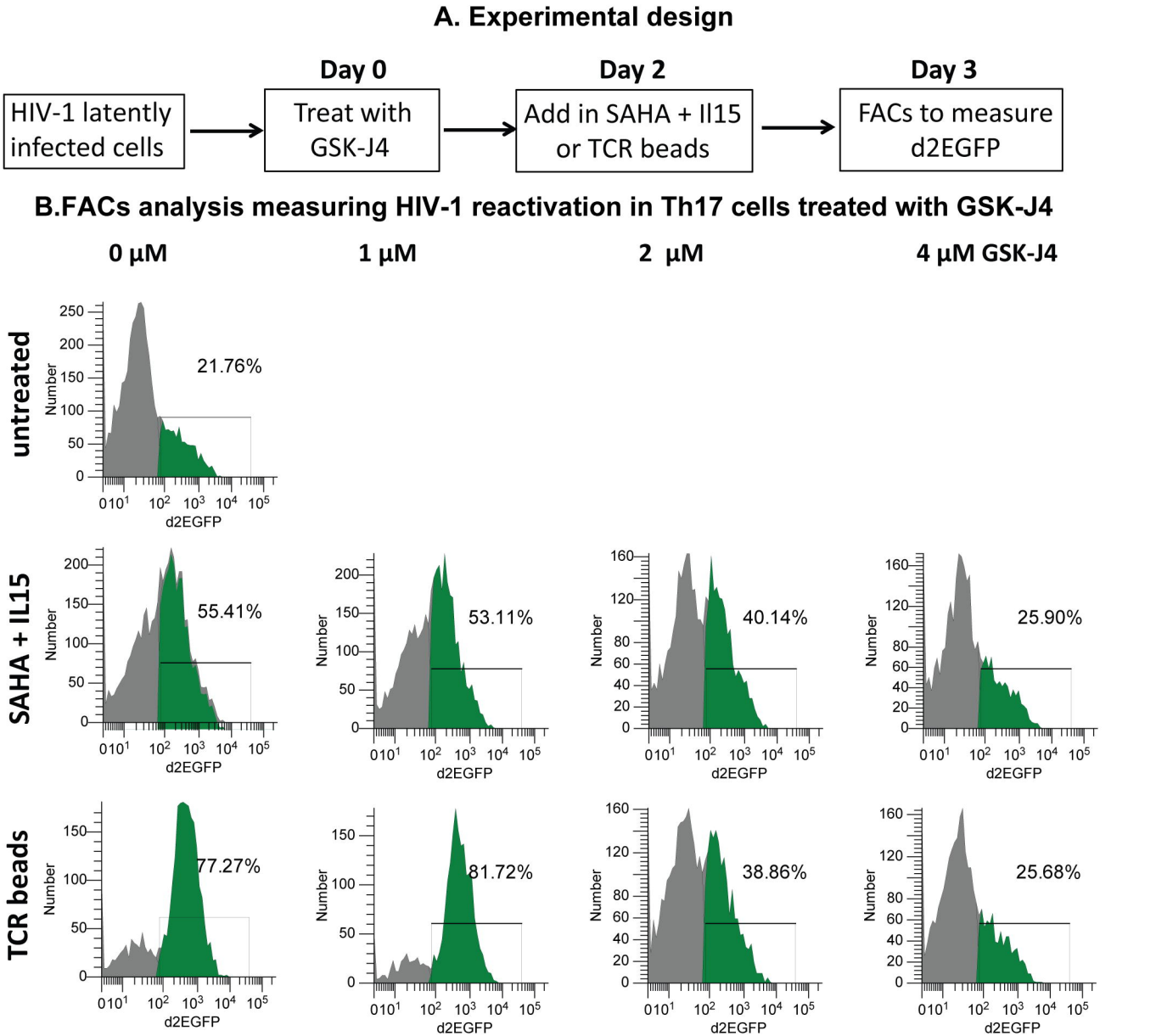
A. Experimental design
Day 0
Day 2
Day 3
HIV-1 latently infected cells
Treat with GSK-J4
Add in SAHA + Il15 or TCR beads
FACs to measure d2EGFP
B.FACs analysis measuring HIV-1 reactivation in Th17 cells treated with GSK-J4
0 µM
1 µM
2 µM
4 µM GSK-J4
untreated
SAHA + IL15
TCR beads
21.76%
55.41%
53.11%
40.14%
25.90%
77.27%
81.72%
38.86%
25.68%
Number
d2EGFP